Marine Micropaleontology, 10 (1986): 235—266
Elsevier Science Publishers B.V., Amsterdam — Printed in The Netherlands

MIDDLE CRETACEOUS CALCAREOUS NANNOFOSSIL BIOGEOGRAPHY AND PRESERVATION IN THE ATLANTIC AND INDIAN OCEANS: IMPLICATIONS FOR PALEOCEANOGRAPHY

PETER H. ROTH and KEITH R. KRUMBACH

Department of Geology and Geophysics, University of Utah, Salt Lake City, UT 84112 (U.S.A.)

(Revised version received January 21, 1985; accepted March 8, 1985)

Abstract

Roth, P.H. and Krumbach, K.R., 1986. Middle Cretaceous calcareous nannofossil biogeography and preservation in the Atlantic and Indian oceans: implications for paleoceanography. Mar. Micropaleontol., 10: 235—266.

The quantitative study of calcareous nannofossil preservation and biogeographic distribution puts constraints on paleoceanographic models for the Atlantic and Indian oceans during the middle Cretaceous. We establish a dissolution ranking of middle Cretaceous calcareous nannofossils based on susceptibility to dissolution. A positive correlation of organic carbon content of the sediments and the relative abundance of *Watznaueria* indicates that much of the carbonate dissolution was caused by the release of carbon dioxide during oxidation of organic matter. The depth distribution of the most dissolution resistant species, *Watznaueria barnesae*, shows relative-abundance maxima at the deepest sites and a maximum where intermediate waters impinge on slopes; this reflects stagnant, oxygen-poor bottom waters and possibly a mid-water oxygen minimum zone with increased deposition and catabolic breakdown of organic matter. Factor analyses are performed on various data sets for three different time slices ranging in age from late Aptian to early Albian, middle Albian and late Albian to Cenomanian. The resulting factors can be related to paleoceanographic conditions such as colder water at high latitudes, high fertility (upwelling conditions) and neritic conditions for all three time intervals. A wide tropical to subtropical zone was flanked by boreal and austral zones. Upwelling conditions probably existed along the North African margin and over the Falkland Plateau. Zonal upwelling is tentatively postulated for the northwestern and northeastern margin of the North Atlantic in the middle Albian and for the eastern margin of the North Atlantic off Western Europe for the late Albian to Cenomanian. We speculate on surface water current patterns, location of upwelling regions and haline-driven deep circulation for the middle Cretaceous.

Introduction

The apparently equable climates and the preservation of organic-carbon-rich marine sediments places interesting constraints on middle Cretaceous paleoceanography.

The existence of widespread, organic-carbon-rich, middle Cretaceous sediments has been attributed to unusual patterns of thermohaline circulation, surface-water productivity, density stratification of the water column, and terrestrial organic carbon input (Roth, 1976, 1978; Schlanger and Jenkyns, 1976; Ryan and Cita, 1977; Thierstein and Berger, 1978; Berger, 1979; Habib, 1979, 1983; Tissot et al., 1979, 1980; Jenkyns, 1980; Brass et al., 1982a). The preservational state of calcareous nannofossils, determined by appearance, species diversity and assemblage composition, reflects the position of the

0377-8398/86/$03.50

sampling site with respect to the calcite compensation depth (CCD) and the total organic carbon content of the sediment. Preservation patterns of calcareous nannofossils put some constraints on models of deep-water circulation for the mid-Cretaceous.

The earth's climate appears to have been more equable with no clear indication of ice-covered poles during the Cretaceous (Schwarzbach, 1974; Frakes, 1979) and only scant evidence for freezing conditions in the Cretaceous seas (Kemper, 1983). We attempt to estimate surface-water temperature patterns from the biogeographic distribution patterns of calcareous nannofossils. Although it is impossible to estimate actual temperatures we can develop a better understanding of water mass distributions and surface-water nutrient concentration from the distribution of calcareous nannofossil assemblages.

Several climatic models for the Cretaceous or post-Paleozoic have been based on continental reconstructions and theoretical considerations or numerical climate models (Barron et al., 1981; Barron and Washington, 1982; Lloyd, 1982; Parrish and Curtis, 1982; Parrish et al., 1982). The last two models have been tested in part against the global distribution patterns of oil and gas source rocks, coals and evaporites. We attempt to provide additional constraints on climatic models based on the paleoceanography inferred from the preservation and distribution of mid-Cretaceous calcareous nannofossils.

We extend the initial coverage by Roth and Bowdler (1981) to include the Indian Ocean but refer the reader to this publication for an overview of previous work on mid-Cretaceous nannoplankton biogeochronology, sea level, calcium carbonate compensation depth, description of sedimentary sections recovered by the Deep Sea Drilling Project and speculations on the origin of black shales.

Samples and methods

Samples from all sections recovered by the Deep Sea Drilling Project that contain mid-Cretaceous calcareous nannofossils were included in this study. A few selected land samples from Britain, southwestern France and Texas were also added. Sampling locations were plotted on paleoreconstructions of Barron and Harrison (1980); this allowed us to determine paleolatitudes of all sites (Fig. 1).

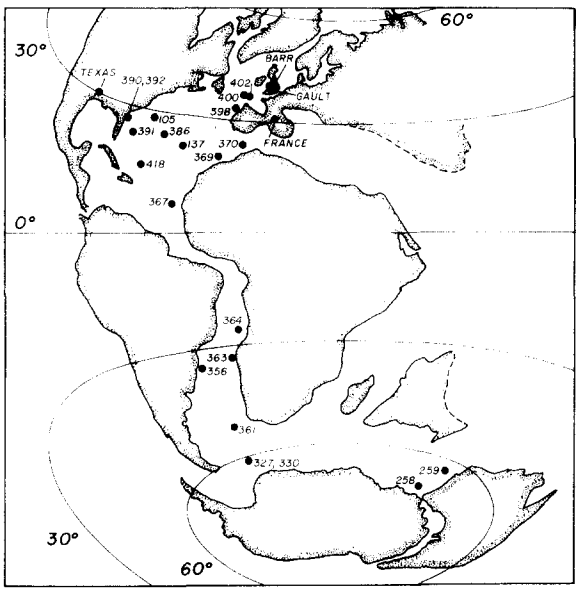

Fig. 1. Site locations and land sections used in this study. (Abbreviations: *Barr* = Barrington Cement Quarry, Cambridgeshire; lower Chalk; *Gault* = Gault Clay, Copt Point, Folkstone, England; *France* = Vocontian Trough, Col de Palluel, Lesches-en-Dois; *Texas* = Duck Creek and Grayson Marl Formations, Grayson County.)

Backtracking of sites was accomplished using techniques discussed by Berger and Winterer (1974) allowing us to estimate paleodepth within an accuracy of about 200 m. Plotting of sedimentary facies on these backtrack curves graphically displays the position of major facies boundaries in a depth framework for the Atlantic and Indian oceans. One of the most important facies boundaries in the oceans is the calcite compensation depth (CCD). It is difficult to determine the exact position of the CCD during the mid-Cretaceous in the Atlantic and Indian oceans (Fig. 2) because of large cyclic fluctua-

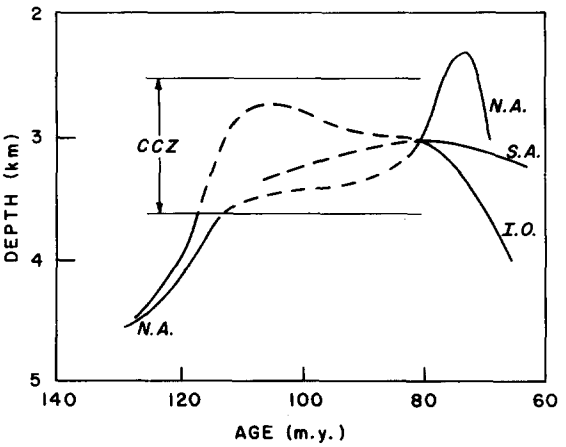

Fig. 2. Carbonate compensation depth (CCD) and carbonate compensation zone (*CCZ*) in the Atlantic and Indian Ocean during the Mesozoic (dashed line: estimate of CCD during time of indistinct CCD).

tions of the calcium carbonate content of the sediments (Thierstein and Roth, 1980; Roth, 1983). However, there is a "calcite compensation zone (CCZ)" that lies between shallower regions where carbonates predominate (shallower than 2.5 km) and a deeper zone where carbonates are missing or rare (below 3.5 km). Sediment redeposition by bottom currents, especially in the western North Atlantic (Kagami et al., 1983) and in the Cape and Angola basins tends to blur this compensation zone even more. We define the CCD for the purpose of our discussions as bisecting the compensation zone. It was thus located at about 3 km depth in the North and South Atlantic and about 2.5 km in the Indian Ocean during the mid-Cretaceous (Fig. 2).

We determined the average carbonate and organic carbon content of a representative set of samples on a LECO Carbon analyzer following the procedures proposed by Heath et al. (1977). Organic carbon contents, carbonate content and linear sedimentation rates for the intervals of interest are summarized as environmental factors by site on Tables I—III. We realize that the number of sections studied is small (fourteen oceanic sections recovered by the Deep Sea Drilling Project and three locations for the land sections) but we used all available oceanic sections and the best land samples in this study.

The sedimentary sections were deposited in different settings. Sites 105 and 418 are in an oceanic setting, i.e., on an abyssal plain or rise far removed from major coarse terrigenous input. Sites 367, 369, 370, 398 and 400 are on the eastern North Atlantic margin and contain some turbidites (Kelts and Arthur, 1981). Sites 390 and 402 are on the upper slope, the former largely isolated from input of terrigenous detritus by a wide carbonate shelf, the latter containing more detrital material. Ridge-crest settings are inferred for Sites 137 and 386 by backtracking. Of the South Atlantic sites, four are on rises and plateaus; 327 and 330 were drilled on the Falkland Plateau; 356, 363 are on the Rio Grande—Walvis Ridge. Site 364 is on the African margin of the Anglo Basin. Of the deep oceanic sites in the Cape Basin, Site 361 contains poorly preserved nannoplankton and Site 530, also in the Cape Basin, contained nannoplankton that were too poorly preserved for quantitative studies (Roth, 1984). The two Indian Ocean sites are located close to the margin of western Australia; Site 258, on the Naturalist Plateau, recovered detrital sediments derived from weathering of basalt and Site 259, on the continental margin off western Australia, contains largely detrital sediments with considerable amounts of pyrite indicative of reducing conditions (Davies and Kidd, 1977).

The lithologies of mid-Cretaceous sediments in both the Atlantic and Indian oceans include clays, nannofossil marls and nannofossil oozes, often finely laminated, sometimes bioturbated. Colors range from gray to greenish gray for deeper abyssal and continental margin sites (105, 137, 327, 330, 356, 361, 363, 367, 369, 370, 386, 398, 400, 402, 418) to red brown and white for shallower, continental margin sites (390, 327, 259). Sediments from the deeper continental margin sites often show lamination, lack burrowing and contain authigenic dolomite, siderite, pyrite and high concentrations (greater than 1%) of organic carbon; this is indicative of reducing conditions at least within the sediments and possibly in the bot-

TABLE I

Environmental factors by site in *Eiffellithus turriseiffeli* Zone (NC 10/11)

Site	Samples per site	Avg. total count	Paleo-depth (m)	Core depth (m)	Sed. rate (m/m.y.)	Paleo-latitude[a]	Carbonate (%)	Organic carbon (%)	Carbon analysis samples
105	3	414	4700	318	5	27°N	23.9	1.3	1
137	25	289	2500	251	15	20°N	35.2	0.7	2
258	5	467	1100	306	45	73°S	24.2	0.4	2
327A	3	355	400	169	18	62°S	48.2	0.7	3
356	3	429	1300	720	3	35°S	42.8	0.2	2
363	5	467	800	537	22	34°S	64.4	1.0	4
364	6	431	1000	754	15	28°S	68.1	0.3	4
367	7	439	4300	691	20	7°N	3.5	10.0	2
369A	2	357	1500	429	13	18°N	34.5	4.7	1
370	13	418	4000	706	12	20°N	10.2	1.0	2
386	9	229	2500	702	22	25°N	60.7	1.3	4
398D	4	463	3000	976	20	33°N	33.1	0.8	2
400A	3	461	3000	658	7	36°N	62.3	0.2	2
418	2	605	2800	259	6	16°N	1.1	1.9	1
Barr.	4	300	100	0	10	40°N	—	—	0
France	3	506	200	0	60	32°N	58.5	0.4	1
Texas	3	308	100	0	12	32°N	—	—	0

[a]At 100 m.y. B.P.

TABLE II

Environmental factors by site in *Deflandrius cretaceus* Zone (NC 8/9)

Site	Samples per site	Avg. total count	Paleo-depth (m)	Core depth (m)	Sed. rate (m/m.y.)	Paleo-latitude[a]	Carbonate (%)	Organic carbon (%)	Carbon analysis samples
258	4	402	1100	395	45	73°S	3.0	1.3	2
259	5	313	2800	131	50	65°S	20.9	0.4	5
327A	7	450	400	238	18	62°S	47.3	0.3	7
330	3	443	400	148	18	62°S	43.5	0.0	2
363	1	447	800	669	22	34°S	74.4	0.3	1
364	2	404	1000	870	24	28°S	80.6	0.4	2
369A	5	406	1500	460	13	18°N	—	—	0
370	3	369	4000	818	12	20°N	13.4	4.6	2
386	3	477	2500	914	22	25°N	—	—	0
390	3	318	150	119	2	24°N	24.7	0.5	2
398D	5	424	2600	1128	20	33°N	17.2	2.1	1
400A	3	467	3000	657	7	36°N	30.9	0.3	1
402A	7	511	1000	293	24	36°N	31.7	1.0	1
418	2	695	2800	274	6	16°N	63.8	0.2	1
France	2	601	200	0	60	32°N	—	—	0
Gault	8	426	100	0	10	38°N	—	—	0
Texas	2	435	100	0	20	30°N	65.9	0.1	1

[a]At 100 m.y. B.P.

TABLE III

Environmental factors by site in *Rhagodiscus angustus* Zone (NC 7)

Site	Samples per site	Avg. total count	Paleo-depth (m)	Core depth (m)	Sed. rate (m/m.y.)	Paleo-latitude[a]	Carbonate (%)	Organic carbon (%)	Carbon analysis samples
327A	1	408	400	338	18	53°S	26.2	2.4	1
361	1	396	3000	1053	29	51°S	0.6	3.9	1
364	1	12	1000	1030	93	28°S	45.0	7.3	1
370	1	393	4000	856	12	20°N	—	—	0
391C	1	324	4400	928	20	28°N	87.0	1.1	1
392A	1	516	150	83	2	24°N	80.0	0.0	1
398D	1	433	2600	1387	25	33°N	2.0	2.0	1
400A	1	468	3000	722	20	36°N	48.0	0.3	1
402A	1	744	1000	454	24	36°N	46.6	0.5	1
418A	1	641	2800	311	6	16°N	—	—	0
France	1	627	200	0	60	32°N	—	—	0
Gault	1	238	100	0	10	38°N	—	—	0

[a]At 100 m.y. B.P.

tom waters too. More detailed descriptions of the sedimentary sections at the various sites can be found in the Initial Reports of the Deep Sea Drilling Project (Hayes and Pimm et al., 1972; Hollister and Ewing et al., 1972; Davies and Luyendyk et al., 1974; Veevers and Heirtzler et al., 1974; Barker and Dalziel et al., 1977; Supko and Perch-Nielsen et al., 1977; Benson and Sheridan et al., 1978; Bolli and Ryan et al., 1978; Lancelot and Seibold et al., 1978; Sibuet and Ryan et al., 1979; Tucholke and Vogt et al., 1979; Donnelly et al., 1980).

Smear slides were studied in the light microscope to determine the preservation of the nannofossils and to determine the exact biostratigraphic position of each sample following the zonation of Roth (1978, 1983). The two zones that were found at the majority of the sites are the *Eiffellithus turriseiffeli* Zone (NC 10) and the *Deflandrius cretaceus* Zone (NC 8). Samples assignable to the *Axopodorhabdus albianus* Zone (NC 9) were included with the ones from the underlying Zone NC 8. In some cases we were uncertain about the upper boundary of Zone NC 10 due to the rarity of *Lithraphidites acutum* and might have included samples from the overlying Zone NC 11 with the ones from Zone NC 10. Thus, in this study we combined the two zones into a single Zone NC 10/11. The *Rhagodiscus angustus* Zone (NC 7) was only recovered in the Atlantic.

The age of the interval NC 10/NC 11 is late Albian to early Cenomanian or Argusian to early Tenerifian (Roth, 1978) and ranges from about 102 m.y. to 92 m.y. B.P. The middle time slice NC 8/NC 9 is of middle Albian or late Magellanian age and covers the interval of about 102—105 m.y. B.P. The oldest time slice, NC 7, is of late Aptian to early Albian or early Magellanian age and covers the time span of 105—109 m.y. B.P. A more thorough discussion of biostratigraphic criteria used in this zonal scheme is found in Roth (1978), Roth and Bowdler (1981) and Roth (1983).

Initial visual estimates of nannofossil preservation using the dissolution/overgrowth scale of Roth (1973) helped us to select samples with moderate to good preservation for quantitative studies. At least 300 specimens were counted by scanning random traverses of the smear slides in the light microscope. Initially, over 100 species were recognized and recorded in the census. To reduce the species list, some closely related species were recombined into larger categories.

Rhagodiscus asper and *R. splendens* were combined; the following groups were listed at the generic level: *Braarudosphaera*, *Broinsonia*, *Gartnerago*, *Cretarhabdus* (also includes species of *Retecapsa*), *Vagalapilla* and *Nannoconus*. Species that never exceeded two percent of the total assemblage were excluded. Thus, we ended up with 20 distinct groups that ac-

TABLE IV

Average census by site of coccolith abundance in *Eiffellithus turriseiffeli*[1] Zone (NC 10/11)

Site	Species																				
	a	b	c	d	e	f	g	h	i	j	k	l	m	n	o	p	q	r	s	t	u
105	6.5	38.2	2.2	8.0	0.2	5.6	3.4	8.0	0.0	3.4	0.0	0.0	1.7	3.4	0.0	0.0	8.0	0.0	0.0	0.0	7.5
137	5.5	15.5	1.0	25.4	2.4	2.4	2.7	5.2	1.0	2.7	1.0	0.0	1.0	5.8	0.0	1.0	5.8	0.0	0.0	0.3	16.2
258	0.6	25.9	0.0	12.8	5.8	1.9	2.4	3.4	1.5	0.2	4.3	15.0	8.1	5.4	0.0	0.0	1.7	1.7	0.0	2.6	5.8
327A	1.1	37.2	0.0	7.0	2.8	0.0	0.0	0.8	4.8	0.3	6.5	24.5	3.4	1.1	0.6	0.3	1.7	0.0	1.1	0.3	5.6
356	7.5	38.2	3.3	6.3	0.5	5.1	2.6	1.9	0.2	4.9	1.2	0.0	0.5	3.7	0.2	0.2	3.3	0.0	0.2	0.5	13.1
363	12.0	23.1	3.0	4.9	1.5	1.7	3.9	7.5	0.0	5.6	2.8	0.0	0.9	2.4	1.7	0.4	1.9	0.0	1.5	1.1	14.3
364	4.9	27.4	1.9	27.1	1.2	2.6	1.6	2.6	0.5	0.7	0.5	0.0	0.2	5.1	0.0	0.5	3.2	0.0	0.7	0.7	14.8
367	8.9	9.1	0.9	20.5	5.7	3.0	4.3	11.6	0.7	1.6	1.6	0.0	0.9	3.6	0.0	1.8	3.4	0.2	0.0	6.8	12.3
369A	2.2	7.3	4.2	21.3	2.0	3.6	3.6	29.4	0.3	2.5	1.1	0.0	3.9	1.4	0.0	0.6	1.7	0.0	0.0	1.4	13.2
370	5.3	18.7	1.4	21.5	2.6	3.3	3.6	14.4	0.7	2.6	0.2	0.0	0.5	3.8	0.0	0.7	3.8	0.0	0.0	1.7	11.7
386	10.9	36.4	0.8	8.5	1.9	3.9	4.3	3.1	0.4	1.2	0.4	0.0	0.4	3.1	0.0	0.4	9.3	0.0	0.0	1.6	10.1
398D	3.2	17.1	3.2	25.5	1.1	3.5	2.8	11.4	0.2	2.6	0.4	0.0	0.4	3.9	0.0	0.6	6.0	0.2	0.0	1.3	14.3
400A	5.6	25.6	4.1	18.0	1.7	4.1	4.3	6.9	0.4	1.7	1.5	0.0	1.5	3.0	0.0	0.2	4.6	0.2	0.0	1.5	12.8
418	16.5	31.2	1.8	6.1	0.3	6.8	2.3	6.0	0.3	1.2	0.0	0.0	1.0	3.0	0.0	0.0	10.4	0.0	0.0	0.8	9.1
Barr.	3.7	40.3	1.0	8.3	2.0	6.0	3.7	2.3	1.0	0.3	9.0	0.3	1.0	3.3	0.0	2.3	3.0	0.0	2.0	5.0	5.7
France	9.1	34.8	1.4	10.1	2.2	4.2	1.6	4.2	0.4	1.4	4.9	0.0	1.2	4.3	0.2	1.2	3.2	0.0	1.2	1.0	10.9
Texas	6.8	14.6	1.3	22.7	1.9	4.9	2.3	3.2	0.6	2.3	1.6	0.0	1.3	4.5	0.3	2.3	5.5	0.0	2.9	4.9	13.6

a: *Rhagodiscus asper/splendens*. b: *Watznaueria barnesae*. c: *Lithraphidites carniolensis*. d: *Biscutum constans*. e: *Deflandrius cretaceus*. f: *Zygodiscus diplogrammus*. g: *Z. elegans*. h: *Z. erectus*. i: *Lithrastrinus floralis*. j: *Discorhabdus ignotus*. k: *Tranolithus orianatus*. l: *Seribiscutum primitivum*. m: *Zygodiscus spiralis*. n: *Eiffellithus turriseiffeli*. o: *Braarudosphaera* spp. p: *Broinsonia* spp. q: *Cretarhabdus* spp. r: *Gartnerago* spp. s: *Nannoconus* spp. t: *Vagalapilla* spp. u: Other spp.

[1] Environment factors by site are shown in Table I.

TABLE V

Average census by site of coccolith abundance in *Deflandrius cretaceus*[1] Zone (NC 8/9)

Site	Species																				
	a	b	c	d	e	f	g	h	i	j	k	l	m	n	o	p	q	r	s	t	u
258	3.0	38.6	0.0	3.5	1.0	1.2	1.7	2.5	0.5	0.2	1.5	29.9	3.5	0.0	0.0	0.2	5.5	0.0	0.0	2.2	4.2
259	1.9	42.8	0.0	11.2	10.9	3.8	1.9	0.6	2.6	0.3	2.9	2.6	1.6	0.0	0.0	0.0	2.2	1.0	0.0	3.2	9.3
327A	6.9	29.8	0.9	12.7	0.2	3.6	2.2	4.9	1.1	2.7	4.2	3.8	4.7	0.0	1.8	1.1	2.7	0.0	1.6	4.4	8.9
330	4.3	45.6	0.7	12.4	0.5	0.2	1.4	2.3	1.1	1.4	0.0	1.6	0.2	0.0	2.7	2.3	4.7	0.0	0.9	5.6	10.2
363	9.6	33.3	3.1	11.6	0.4	0.4	3.6	3.4	0.0	4.3	2.0	0.0	1.3	0.0	2.7	0.4	4.7	0.0	0.16	0.9	11.2
364	11.6	42.3	2.7	6.4	0.7	10.1	3.2	4.0	0.0	3.5	1.0	0.0	1.0	0.0	0.5	0.5	2.2	0.0	0.0	1.0	7.7
369A	5.2	8.9	3.9	24.6	1.7	3.0	5.2	24.6	0.5	2.0	0.2	0.2	1.5	0.0	0.0	0.7	1.7	0.0	0.0	2.2	12.3
370	10.3	26.0	5.7	6.5	0.5	6.2	6.8	13.6	0.5	1.4	0.0	0.0	0.3	0.0	0.0	0.0	1.6	0.0	0.0	5.4	8.1
386	10.3	30.6	3.6	5.7	0.8	2.3	2.3	15.7	0.6	5.5	0.6	0.0	0.8	0.0	0.0	0.0	2.7	0.0	0.0	2.7	11.7
390	8.7	17.4	7.4	16.6	2.5	2.2	3.0	15.3	0.8	2.7	0.5	0.0	0.5	0.0	1.1	0.3	2.5	0.0	1.4	1.9	13.6
398D	5.7	25.5	4.5	13.4	0.7	3.1	5.0	15.8	0.5	2.4	0.0	0.0	1.2	0.0	0.2	0.0	3.8	0.2	0.2	1.2	12.0
400A	7.3	30.8	7.7	11.6	1.5	3.0	5.1	9.0	0.2	1.5	0.2	0.0	1.1	0.0	0.0	0.0	3.9	0.0	0.0	1.9	12.4
402A	10.0	18.4	7.0	4.5	0.4	2.9	5.1	12.9	0.2	2.3	0.0	0.0	0.6	0.0	0.4	0.0	2.0	0.0	17.8	3.3	9.8
418	11.8	22.7	10.2	8.9	2.0	2.0	2.3	10.8	1.0	2.0	0.0	0.0	1.4	0.0	0.0	0.0	2.4	0.0	0.0	2.4	13.8
France	10.1	48.8	2.0	6.3	1.0	3.0	2.3	8.5	0.7	1.5	0.7	0.0	0.5	0.0	0.0	0.2	2.2	0.0	0.7	1.5	6.5
Gault	8.2	35.7	1.2	6.1	3.1	7.3	8.0	10.1	0.7	0.2	0.2	0.7	0.9	0.5	0.0	0.2	2.1	0.0	0.0	4.5	8.5
Texas	11.0	21.1	2.5	8.5	1.4	3.7	3.2	10.6	1.4	2.3	2.1	0.0	1.1	0.0	2.1	0.9	4.4	0.0	9.7	2.3	11.7

a: *Rhagodiscus asper/splendens*. b: *Watznaueria barnesae*. c: *Lithraphidites carniolensis*. d: *Biscutum constans*. e: *Deflandrius cretaceus*. f: *Zygodiscus diplogrammus*. g: *Z. elegans*. h: *Z. erectus*. i: *Lithrastrinus floralis*. j: *Discorhabdus ignotus*. k: *Tranolithus orianatus*. l: *Seribiscutum primitivum*. m: *Zygodiscus spiralis*. n: *Eiffellithus turriseiffeli*. o: *Braarudosphaera* spp. p: *Broinsonia* spp. q: *Cretarhabdus* spp. r: *Gartnerago* spp. s: *Nannoconus* spp. t: *Vagalapilla* spp. u: Other spp.

[1] Environmental factors by site are shown in Table II.

TABLE VI

Percentage of coccolith abundance by site in *Rhogodiscus angustus*[1] Zone (NC 7)

Site	Species												
	a	b	c	d	e	f	g	h	i	j	k	l	m
327A	27.0	37.5	0.7	3.2	1.0	2.7	3.4	1.0	0.0	0.5	0.0	3.4	20.1
361	18.7	58.6	0.0	0.5	0.0	0.5	0.8	0.0	0.0	0.0	0.0	1.3	19.6
364	0.0	83.0	0.0	0.0	0.0	0.0	0.0	0.0	0.0	0.0	0.0	0.0	16.7
370	5.1	27.5	4.3	2.0	4.3	14.0	12.2	0.0	0.0	0.0	0.0	4.8	25.8
391C	18.8	29.6	10.2	0.6	1.2	4.6	4.0	0.0	0.9	0.0	3.7	2.5	23.9
392A	7.2	27.1	7.2	1.4	0.6	1.4	3.5	0.0	1.9	0.0	32.6	2.1	15.0
398D	3.2	31.2	6.2	6.2	1.8	5.5	19.2	0.7	0.0	0.0	0.5	3.2	22.3
400A	8.1	30.8	7.1	15.4	1.5	2.1	9.6	0.9	0.0	0.0	1.1	1.9	21.5
402A	10.8	14.1	6.5	5.2	1.1	2.3	9.0	0.4	1.4	0.0	35.9	0.5	13.0
418A	8.9	33.9	11.1	1.2	0.8	2.5	14.5	0.5	0.0	0.0	0.0	1.6	25.0
France	16.3	27.9	4.0	3.8	2.4	1.6	18.5	0.0	0.5	0.0	7.8	1.4	15.8
Gault	6.7	71.4	1.3	0.8	0.8	1.3	5.5	0.0	0.0	0.0	0.0	1.7	10.5

a: *Rhagodiscus asper/splendens.* b: *Watznaueria barnesae.* c: *Lithraphidites carniolensis.* d: *Biscutum constans.* e: *Zygodiscus diplogrammus.* f: *Z. elegans.* g: *Z. erectus.* h: *Z. spiralis.* i: *Braarudosphaera* spp. j: *Broinsonia* spp. k: *Nannoconus* spp. l: *Vagalapilla* spp. m: Other spp.

[1] Environmental factors by site are shown in Table III.

counted for 85—95% of the specimens in each sample. Of these 20 groups 11 showed considerable spatial variability. The Tables IV—VI list nannofossil counts and percentages of all samples at each site used in this study.

Various multivariate statistical techniques were used in an exploratory study, including *R*-mode and *Q*-mode cluster analysis, *R*-mode and *Q*-mode factor analysis and canonical correlation analysis. We report here mainly on the technique that provided the most consistent results, namely *R*-mode factor analysis with varimax rotation (Nie et al., 1975). We did invert the data matrix and apply the same factor analysis program to obtain a *Q*-mode factor analysis but the results were less conclusive.

Factor analysis is a robust statistical technique requiring data which at least approach normal distribution. All possibly acceptable samples were used rather than the single best sample for the two younger time slices. As the number of samples is increased, the distribution tends towards normality (central limit theorem) thereby improving the viability of the technique. Because of the limited data only a set of the best preserved samples was used for time slice NC 7 (see Tables III and VI).

Preservation of calcareous nannofossils

Middle Cretaceous strata in the Atlantic and Indian oceans contain a dearth of calcium carbonate compared to the underlying lower Cretaceous strata. The "calcite compensation zone" shallowed by about two kilometers from the early to the late Cretaceous (Fig. 2). This affected the preservation of nannofossil assemblages in the sediments. Pristine samples are almost never observed except at the shallowest sites. The great majority of the samples show slight to moderate dissolution effects. Some samples, especially in the deepest basin locations, contain poorly preserved (strongly etched) nannofossils. High organic carbon content in sediments adversely affects the preservation of coccoliths. Breakdown of organic carbon by bacteria increases the dissolved carbon dioxide content of pore waters

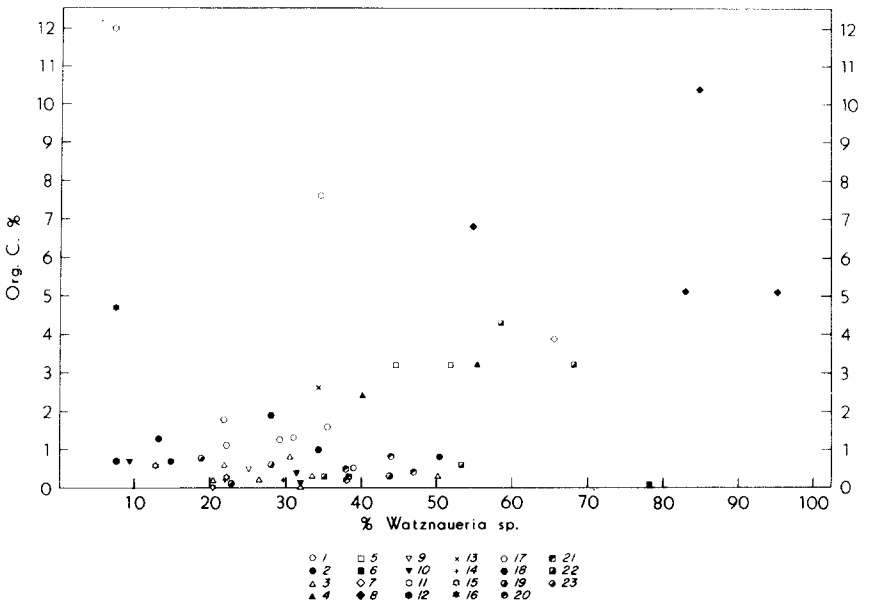

Fig. 3. Relative abundance of *Watznaueria* spp. (a measure of carbonate dissolution) versus percent of organic carbon, NC 10/11, Deep Sea Drilling Project Sites in the Atlantic and Indian oceans. Both symbols and numbers indicate sites (i.e. 105) and zones (i.e. NC 10): *1*=105, NC 10; *2*=327A, NC 10; *3*=327A, NC 8; *4*=327A NC 7; *5*=327A, NC 5/6; *6*=361, NC 8; *7*=361, NC 7; *8*=361, NC 5/6; *9*=363, NC 10; *10*=364, NC 10; *11*=367, NC 10/11; *12*=370, NC 10/11; *13*=391C, NC 8; *14*=400A, NC 10/11; *15*=398D, NC 10/11; *16*=369A, NC 10; *17*=386, NC 10; *18*=418A, NC 10; *19*=258, NC 8; *20*=259, NC 8; *21*=363, NC 8; *22*=364, NC 8/9; *23*=258, NC 10.

and results in carbonate dissolution. A plot of organic carbon versus the relative abundance of *Watznaueria*, the most dissolution resistant genus of mid-Cretaceous nannofossils, shows a positive correlation; thus, dissolution appears more extensive in organic-carbon-rich sediments (Fig. 3). Exceptions to this trend are samples from Sites 367 and 369; they contain high organic carbon contents but low relative abundances of *Watznaueria barnesae*. We invoke relatively high organic carbon accumulation rates and rapid burial of organic matter, thus reducing the amount of catabolically produced carbon dioxide in pore waters and resulting in good overall preservation of the coccoliths. An alternative explanation of contributing factors would be shallow sulfate reduction with concomitant alkalinity increase. Our samples from Sites 327 on the Falkland Plateau, Site 259 off western Australia and some samples from Sites 258, 361 and 364 show much reduced organic carbon values and thus lie below the general trend perhaps because initial organic carbon contents were not very high and much of the organic carbon was totally used up by oxidation within the sediment. Therefore, carbonate dissolution was intense and remaining organic carbon contents are low.

The position of the boundary of oxygen rich and anoxic or dysaerobic waters plays also an important role in carbonate preservation. If sulfate reduction occurs at the sediment—water interface, the alkalinity can increase sufficiently to preserve calcium carbonate; if sulfate reduction takes place within the interstitial waters below the sediment surface, the alkalinity increase comes too late (Berger, 1979). The presence of pyrite in many mid-Cretaceous sediments demonstrates the importance of sulfate reduction. Cyclic changes in carbonate content are indicative of possible fluctuations of the upper boundary of sulfate reduction in the

sediment during the middle Cretaceous. Input of carbonate-rich and organic-carbon-rich sediments by turbidity currents also appears to have been important in distributing carbonate and organic carbon along the continental margins (Dean and Gardner, 1982). We are only beginning to understand these important chemical changes in the mid-Cretaceous sediments during early diagenesis.

Dissolution ranking and dissolution patterns

Coccolith preservation is a very delicate indicator of carbonate dissolution and recrystallization and combined with sedimentological and geochemical data contributes to a better understanding of the processes of cyclic black shale formation. Semiquantitative estimates of preservation (Roth and Thierstein, 1972; Roth, 1973) still give among the most reliable estimates of preservation. We also used dissolution rankings similar to the ones applied to recent coccoliths in Roth and Berger (1975) to attempt a more quantitative dissolution ranking for mid-Cretaceous coccoliths. Such dissolution rankings work best for large data sets from oceanic regions where water depth of samples is well defined and continental-margin effects are unimportant. Where dissolution is more pronounced and where continental-margin effects (e.g. increased organic production and redeposition) are more important (such as in the modern North Pacific) coccolith dissolution indices and dissolution rankings often lack consistent patterns (Roth and Coulbourn, 1982). The situation for our mid-Cretaceous data set is even worse. Dissolution was intense, sample coverage is small and many sites are on continental margins. Paleodepth reconstructions are not very reliable for many sites. The small number of sites precludes rigid latitudinal limitations for the comparison of sites during the dissolution ranking procedures. Thus, paleoenvironmental variables such as surface water temperature, salinity and nutrient concentration introduce much noise and distortion in our analysis of nannofossil preservation. In the dissolution ranking analysis presented here (Tables VII and VIII) we used the best preserved samples from the two time-slices (Zones NC 10/11 and NC 8/9) for which the sample coverage was sufficient and which had been used previously for the biogeographic studies by

TABLE VII

Dissolution ranking and normalized scores for species that formed at least 20 pairs, NC 10/11

Rank	Species	Score
1.	*Watznaueria ba[illegible]e*	26.90
2.	*Zygodiscus ele[illegible]*	15.00
3.	*Deflandrius cretaceus*	12.50
4.	*Watznaueria supracretacea*	1.50
5.	*Eiffellithus turriseiffeli*	0.36
6.	*Tranolithus gabalus*	−2.38
7.	*Zygodiscus diplogrammus*	−2.59
8.	*Lithraphidites carniolensis*	−4.84
9.	*Manivitella pemmatoidea*	−7.92
10.	*Zygodiscus spiralis*	−8.70
11.	*Zygodiscus erectus*	−12.42
12.	*Cretarhabdus* spp.	−14.83
13.	*Rhagodiscus asper/R. splendens*	−22.33
14.	*Biscutum constans*	−37.27

TABLE VIII

Dissolution ranking and normalized scores for species that formed more than 27 pairs

Rank	Species	Score
1.	*Lithraphidites carniolensis*	18.00
2.	*Watznaueria ovata*	15.88
3.	*Watznaueria barnesae*	13.54
4.	*Vagalapilla stradneri*	13.00
5.	*Watznaueria supracretacea*	12.86
6.	*Rhagodiscus asper/R. splendens*	10.00
7.	*Zygodiscus diplogrammus*	7.50
8.	*Cyclagelosphaera margerelii*	3.79
9.	*Discorhabdus ignotus*	0.69
10.	*Vagalapilla matalosa* *Stephanolithus laffittei*	−1.33
11.	*Watznaueria biporta*	−2.22
12.	*Cretarhabdus* spp.	−3.17
13.	*Chiastozygus litterarius*	−3.71
14.	*Prediscophaera cretacea*	−4.67
15.	*Rhagodiscus angustus*	−10.00
16.	*Zygodiscus erectus*	−11.49
17.	*Zygodiscus elegans*	−11.90
18.	*Biscutum constans*	−13.19

Roth and Bowdler (1981). The upper Albian (NC 10/11) sample set contains 14 samples from the following DSDP Sites: 400A, 105, 391, 370, 367, 356, 363, 327A, 398D, 369A, 137, 418, and one sample from southern France (Col de Pallule Section; Thierstein, 1973). The older data set of middle Albian (NC 8/9) age contains 18 samples from the same DSDP Sites as above (excepting Sites 105 and 391 and adding samples from Sites 390, 392 and 386A) and different land samples, namely from the Gault Clay at Folkstone, U.K., the Hautes-Alpes Section of southeastern France and the Albian of Texas, U.S.A. Paleodepth was selected as the sole criterion for discriminating better preserved and more poorly preserved samples in the ranking procedure (for details see Roth and Berger, 1975). The latitudinal distance limit for sample comparison was set at 20°. Scores were normalized by dividing them by the number of pairs that were formed. Only scores of species that formed more pairs than there were samples in the set were considered meaningful and are listed from the most solution-resistant at the top to the least dissolution resistant ones at the bottom, or more precisely from species that showed greater abundances at sites of greater paleodepth than at sites of shallow paleodepth (Tables VII and VIII). Paleogeographic effects could not be excluded completely and are responsible for some of the anomalous rankings compared with other studies (Hill, 1975; Thierstein, 1980).

Details of the dissolution rankings are not always meaningful as a comparison of the two rankings shown here clearly demonstrates. Only the general position of the more common species in a rank list, i.e., whether it is susceptible or resistant or intermediate, seems to be reproducible with different data sets or experimental approaches. Our investigation of nannofossil assemblages in several hundred middle Cretaceous samples indicate that the following species are dissolution resistant: *Watznaueria barnesae*, *W. ovata*, *W. oblongata*, *Deflandrius cretaceus*, *Eiffellithus turriseiffeli*, *Cretarhabdus* spp. and *Retacapsa* spp. Dissolution susceptible species are *Zygodiscus* spp. and *Chiastozygus litterarius*. All other species show intermediate susceptibility to dissolution. The dissolution ranking presented here shows that most of the species listed above fall in the right position in our dissolution ranking. *Lithraphidites carniolensis* and *Zygodiscus elegans* show variable position in the rankings for two time slices. *Biscutum constans* appears in the wrong position in our rankings; it appears to be more dissolution resistant than its rank would imply. Our data set was too small for an entirely reliable dissolution ranking; paleolatitude and continental margin effects (upwelling, redeposition) biased the dissolution ranking. Thus, we did not calculate dissolution indices for the samples (see e.g. Roth and Berger, 1975). Instead we have plotted maximum abundance of *Watznaueria barnesae* versus depth to test the relationship of preservation versus depth (Fig. 4). This plot shows that preservation patterns are complex. There appears to be a steady increase of *W. barnesae* with depth for North Atlantic open ocean sites. However, continental margin sites show smaller overall relative abundance. Secondary overgrowth in pure carbonate sediments resulted in a relative increase in *Watznaueria barnesae* because

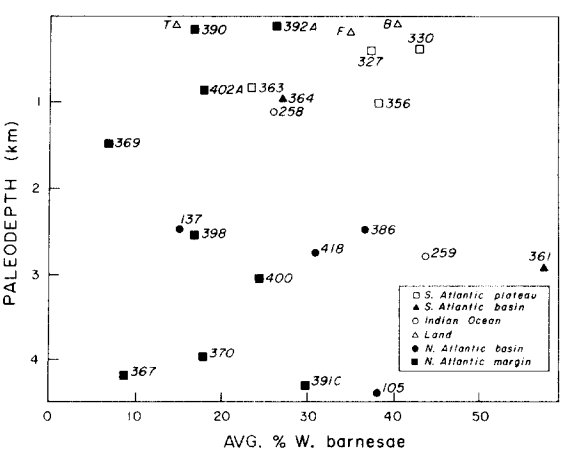

Fig. 4. Relative abundance of *Watznaueria barnesae*, average for each site, versus paleodepth, NC 10/11, Atlantic, Indian oceans and adjacent epeiric seas.

more delicate forms become unrecognizable. There is a slight indication of a mid-depth relative-abundance peak which would mean increased dissolution for sites centered around 2.5 km water depth which might be related to a mid-water oxygen minimum zone with increased organic carbon input resulting in dissolution due to breakdown of organic matter in the sediment (Fig. 4). The distribution of the most dissolution resistant nannofossil species with depth clearly shows the lack of a clear depth gradient of dissolution and lends further support to our observation that the mid-Cretaceous compensation zone is rather broad and a sharp CCD is absent. However, there are also indications of different carbonate dissolution patterns for different ocean basins with more intense dissolution in the South Atlantic and Indian oceans and less pronounced dissolution in the North Atlantic.

The relative abundance of *Watznaueria* is not only affected by dissolution but also by other paleoenvironmental parameters. Thus, we use an additional measure of preservation, namely species diversity. Our study of hundreds of samples has shown that the best preserved samples generally contain the most diverse nannofossil assemblages. We determined both the maximum and mean diversity of all samples from a particular time slice at each site. Distribution patterns of mean diversity are very similar and thus only maximum diversity is shown here plotted in a depth/latitude framework and on a paleoreconstruction map (Fig. 5A,B). There is neither a clear correlation between diversity and depth nor between diversity and latitude. However, deepest sites do show lowest diversities and assemblages are thus considered most dissolved. There does not appear to be a sharp break in species diversity at any particular depth thus supporting the idea that there was an extensive calcite compensation zone rather than a sharp CCD. Lower diversity values between 2 and 3 km, especially at oceanic sites are consistent with the model of a mid-water oxygen minimum zone with increased dissolution. The geographic pattern of diversity shows highest values and thus best

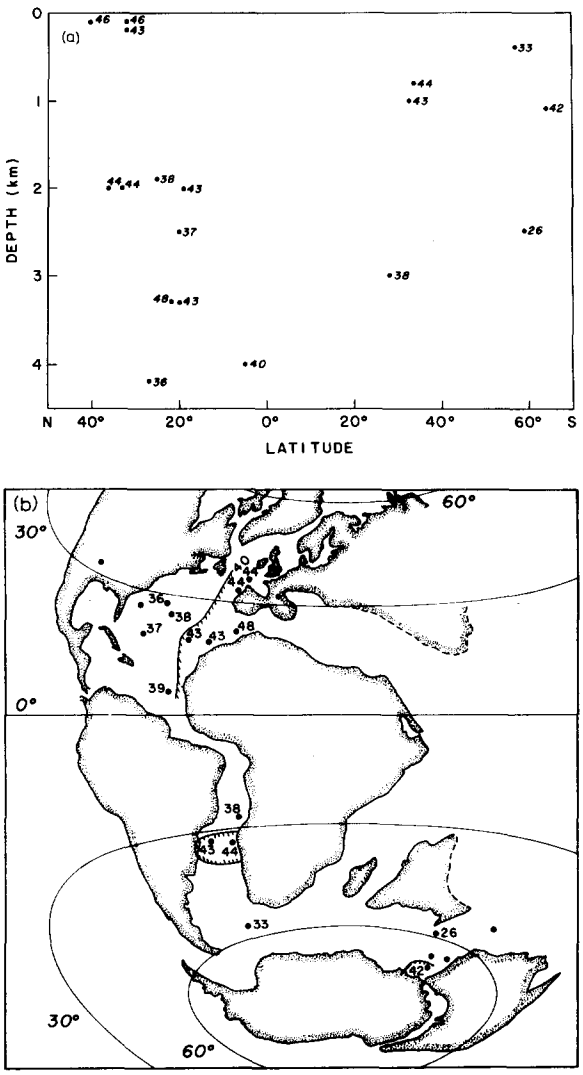

Fig. 5.a. Maximum total nannofossil species diversity for each location versus paleodepth, NC 10/11. b. Geographic distribution of maximum species diversities, NC 10/11. Hatchured areas indicate highest diversity.

preservation along the eastern margin of the Atlantic, on the Rio Grande—Walvis Ridge, Broken Ridge and in epicontinental seas. However, the range of diversities is not very great and thus dissolution is not a major factor in explaining the observed species distribution patterns. Diversity plots for older time slices are similar and are thus not shown here.

Discussion of nannofossil preservation

Calcareous nannofossil preservation patterns in middle Cretaceous sediments of the Atlantic and Indian oceans are complex. Dissolution was most intense in the deep basins of the Northwest Atlantic (Sites 105, 391). At some deep basin sites, such as Site 534 in the Blake Bahama Basin, calcareous nannofossils of Albian age have been almost totally dissolved and are only found in a few thin layers, together with numerous carbonate laths. These thin layers may have been deposited as turbidites that had their source at shallower depths (Roth, 1983). Similar conditions existed in the Cape and Angola basins of the South Atlantic (Sites 361 and 530; see Roth, 1984) where calcareous nannofossils are very poorly preserved or absent from middle Cretaceous sediments that appear to be mostly distal turbidites.

Dissolution of carbonate at these deep water sites appears to be largely due to the presence of relatively old, sluggish high-salinity deep waters enriched in carbon dioxide produced by decay of organic matter introduced by high surface productivity and also added by turbidity currents from sources on the shelf and upper slope. Shallower sites, such as the ridge-crest Site 137 show good preservation. Surface-water productivity in the waters overlying this open-ocean site was lower than along the continental margin and organic-carbon-rich turbidites did not reach this site. However, there appears to be a mid-water zone of poor preservation – centered around 2.5 km water depth which was especially pronounced in the North Atlantic, in particular the western basin. This is reflected in a great increase in the relative abundance of *Watznaueria barnesae* and in reduced diversities at Sites 386 and 418 (Fig. 5A,B). This mid-water dissolution peak could have been caused by an intermediate water oxygen-minimum zone and associated high organic carbon accumulation in regions of surface current shear that resulted in carbon dioxide produced by bacterial action within the sediment. Another possible explanation is the advection of oxygen-depleted waters from an oxygen-minimum zone in the eastern Pacific (Tissot et al., 1979).

Along the continental margins of the southeastern North Atlantic, complicated oceanographic and sedimentation patterns existed. Production of marine organic matter was high (Tissot et al., 1979, 1980). Cyclic turbidity current activity added organic matter which in turn affected the redox conditions in the sediments (Dean and Gardner, 1982). We observe considerable fluctuations in the preservation of calcareous nannofossils at these sites periodically.

In the South Atlantic, dissolution was intense even at shallow sites (Sites 356, 363, 327). This was probably caused by upwelling conditions as nutrient-rich waters from the narrow sea were forced to rise above these shallow plateaus.

Along the western coast of Australia nannofossil preservation is generally poor, especially at the deeper Site 259, and cyclic changes in preservation are observed at both Site 258 and 259.

Detailed studies of coccolith preservation in mid-Cretaceous black shale cycles in the Atlantic (Thierstein and Roth, 1980; Roth, 1983) show that in many of these cycles there is an inverse correlation between nannofossil preservation and organic carbon contents; the dark laminated portions of the sequences have the most poorly preserved coccoliths. Thus, there is a link between organic carbon content and coccolith dissolution in middle Cretaceous sediments (Fig. 3). The origin of these black shale cycles is still somewhat uncertain. Change in upwelling conditions and cyclic organic carbon input by turbidity currents appear to have been important but diagenetic changes greatly altered calcareous nannofossil assemblages. Sulfate reduction could have played an important part in the preservation of carbonate (Berner, 1971; Berger, 1979). If it occurred at or close to the sediment–water interface increased alkalinity in the pore water protected carbonates from dissolu-

tion (Berger, 1979). Cyclic sequences of more carbonate-rich and more organic-rich layers could have been caused by cyclic changes in the upper boundary of sulfate reduction. More detailed studies on the geochemistry and nannofossil preservation need to be completed before we can sort out this complex pattern of carbonate and organic carbon sedimentation.

Preservation patterns of calcareous nannofossils show the major trends of carbonate dissolution and reflect paleodepth, organic carbon production and turbidity current inputs.

Calcareous nannoplankton biogeography

The samples selected for biogeographic studies include only the best preserved assemblages in order to minimize dissolution effects.

During the early phases of the study of mid-Cretaceous biogeographic patterns of all major and some minor species were plotted. Species that show consistent patterns in the Atlantic were identified and their distribution shown in Roth and Bowdler (1981). Multivariate techniques confirmed our initial studies and showed that many of the species that display clear biogeographic patterns are also major variables in the statistically determined groups. Ideally biogeographic analysis should be performed on samples selected from a time plane. This approach was not feasible in the present study because of the limited data set and problems of biostratigraphic resolution. Thus, we chose to use time slices to follow the approach employed by Haq and Lohman (1976). The three time slices are: NC 10/11, *Eiffellithus turriseiffeli* and *Lithraphidites acutum* Zones, late Albian to early Cenomanian, about 102—92 m.y. B.P.; NC 8/9, *Deflandrius cretaceus* and *Axopodorhabdus albianus* Zones, about 102—105 m.y. B.P. and NC 7, *Rhagodiscus angustus* Zone, about 105—109 m.y. B.P. These time slices appear to be the smallest units consistantly resolvable in the present sample set.

Our multivariate statistical analyses of Atlantic and Indian Ocean samples showed the best distribution patterns for time slice NC 10/11 (late Albian/Cenomanian). Patterns are less clear for the middle Albian time slice (NC 8/9) and the early Albian to late Aptian time slice NC 7 and we shall thus pay more attention to the youngest time slice and treat the older time-slices only briefly. Sample coverage for even older time slices such as the early Albian (NC 6) and the late Barremian (NC 5) are insufficient for multivariate statistical analysis and are thus not discussed here.

Time slice NC 10/11

We first show the biogeographic distribution patterns for important species for time slice NC 10/11 (see Figs. 7—9, 11—14) and then discuss the results of a factor analysis for this time slice (see Tables VIII—XI).

In this study we use assemblage diversity as a measure of preservation. Well preserved nannofossil assemblages have the highest species diversity and poorly preserved assemblages are least diverse. The dominant species in most samples is *Watznaueria barnesae*. It is among the most dissolution resistant species and is enriched in poorly preserved assemblages. There is a fairly good linear correlation between diversity and relative abundance of *W. barnesae* (Fig. 6). As a rule, assemblages

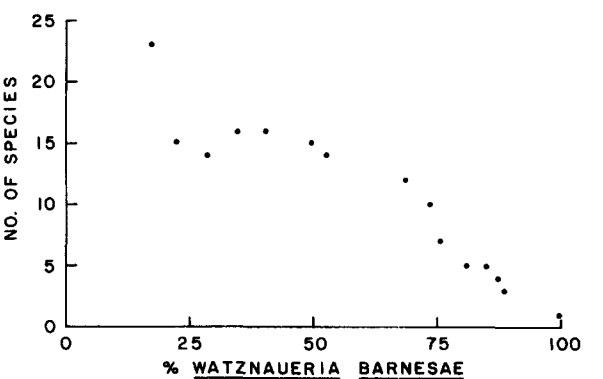

Fig. 6. Relative abundance of *Watznaueria barnesae* versus species diversity (species that comprised more than 1% of a total count of 400 specimens).

with more than 40% *W. barnesae* are too highly dissolved to accurately reflect original species composition and were generally avoided in studies of the nannoplankton biogeography.

Watznaueria barnesae is most abundant in samples from oceanic sites (DSDP Sites 105, 386), some of the sites from the shallow ridges and plateaus in the South Atlantic (Sites 327, 356, 363), and Site 258 in the Indian Ocean (Fig. 7). *Watznaueria barnesae* is least abundant at continental margin sites on the eastern side of the North Atlantic (Sites 367, 369, 370, 398). This confirms our hypothesis that *W. barnesae* is a species that is most abundant in oceanic settings and depleted in high-nutrient ("upwelling") regions during the middle Cretaceous. Land samples of poor preservation (southeastern France, Cenomanian of Great Britain) are generally enriched in *W. barnesae* but well preserved samples from marly samples (Texas) show lower abundances. Carbonate dissolution tends to secondarily enrich this form in poorly preserved assemblages and thus great

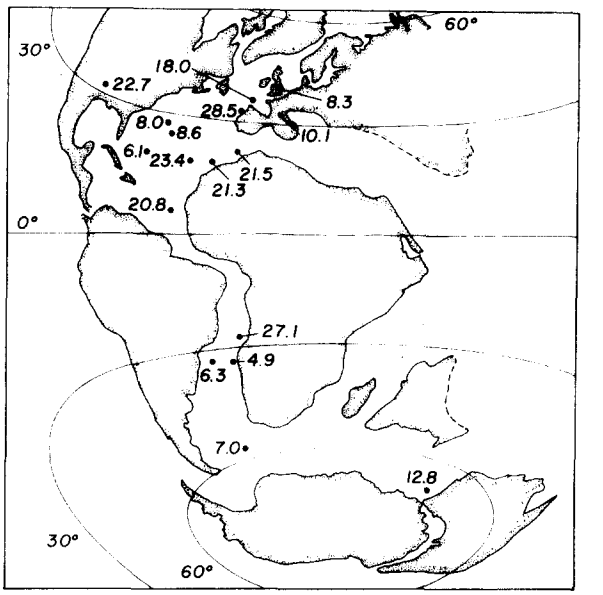

Fig. 8. Biogeographic distribution of *Biscutum constans* plotted as average relative abundance (%) at sites in the Atlantic, Indian oceans and adjacent seas, NC 10/11.

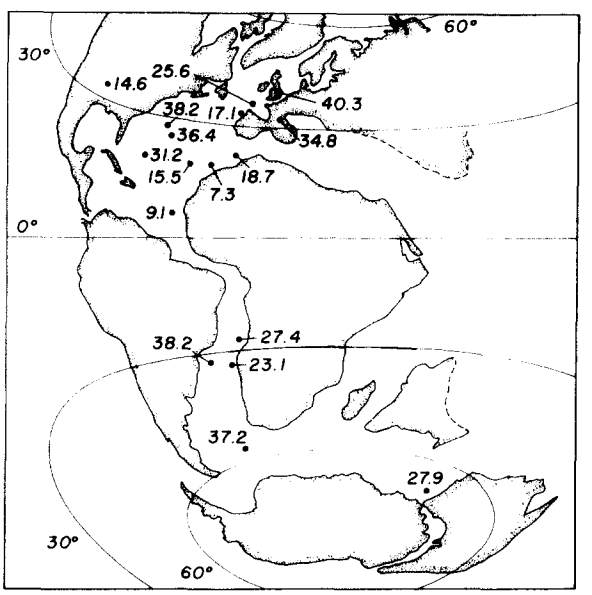

Fig. 7. Biogeographic distribution of *Watznaueria barnesae* plotted as average relative abundance (%) at sites in the Atlantic and Indian oceans and adjacent seas, NC 10/11.

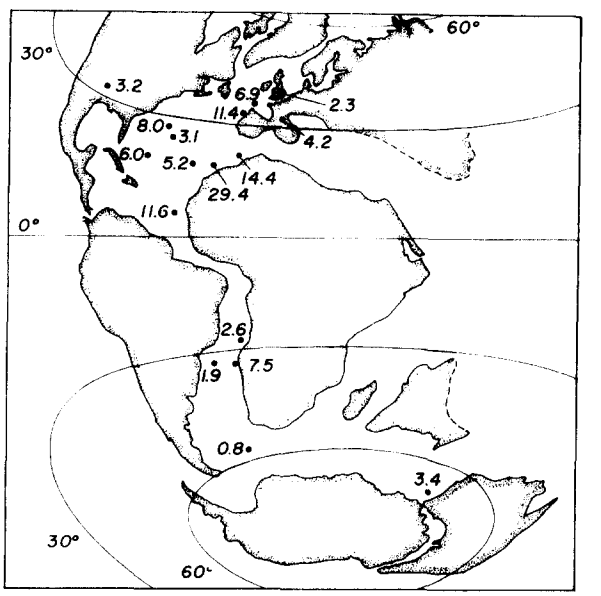

Fig. 9. Biogeographic distribution of *Zygodiscus erectus* plotted as average relative abundance (%) at sites in the Atlantic, Indian oceans and adjacent seas, NC 10/11.

care is required to exclude such assemblages from biogeographic studies.

Biscutum constans (Fig. 8) and *Zygodiscus erectus* (Fig. 9) show distribution patterns that are almost the opposite of *W. barnesae*. Both species are most abundant along the eastern continental margin of the North Atlantic (Sites 367, 369, 370, 398, 400). *Biscutum constans* is most abundant in some of the samples from the Angola Basin (Site 364) but *Zygodiscus erectus* is not particularly abundant at this site, possibly because of dissolution. *Biscutum constans* is also abundant in the epicontinental deposits in Texas but only moderately abundant in southeastern France because of poor preservation. At oceanic sites, with the exception of a shallow ridge-crest site (Site 137), *B. constans* and *Z. erectus* are less abundant than along eastern margins of the Atlantic. Following earlier speculations of Roth and Bowdler (1981) and Roth (1981), we consider *B. constans* and *Z. erectus* as indicators of high surface-water fertility ("upwelling") along eastern margins of ocean basins and divergences (Roth, 1981).

A plot of the relative abundance of *Watznaueria barnesae* versus *Biscutum constans* plus *Zygodiscus* spp. (Fig. 10) allows us to group the various sites into three groups. Sites along the eastern Atlantic margin have high relative abundances of *Biscutum constans* plus *Zygodiscus* spp. but low abundances of *Watznaueria barnesae* and are here interpreted as high fertility ("upwelling") sites (Fig. 10). Oceanic sites from the western North Atlantic and Plateau sites from the South Atlantic form a distinctive group of sites that include oceanic sites and poorly preserved land samples. An intermediate group includes Sites 400 and 137 in the North Atlantic, Site 364 in the Angola Basin and well preserved epicontinental sea deposits from Texas (Fig. 10). Although we showed above that preservational changes affect the relative abundance of the three species used here paleofertility appears to have been the overriding factor affecting the distribution of these species.

Two genera are indicative of neritic or

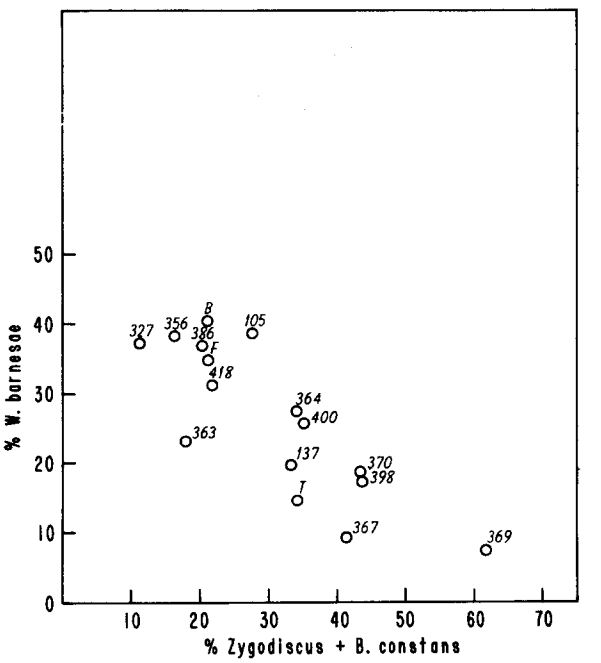

Fig. 10. Relative abundance of *Watznaueria barnesae* versus the sum of relative abundances of *Zygodiscus* spp. and *Biscutum constans*; average relative abundances (%) for all three species; NC 10/11. (Abbreviations: *B* = Barrington Cement Quarry; *F* = France, Vocontian Trough; *T* = Texas.)

shallow continental margin and epicontinental sea conditions, *Broinsonia* and *Nannoconus*. They are most abundant in Texas, the English Chalk and in southeastern France (Figs. 11 and 12). *Broinsonia* is also moderately common at shallow ridge sites (Site 137) and at one continental margin site (Site 367, Fig. 11). *Nannoconus* is fairly abundant on the shallow Falkland Plateau (Fig. 12). These distribution patterns show that shallow water depth and proximity to continents, but not necessarily upwelling condition, favor the presence of *Broinsonia* and *Nannoconus*. Because both species are generally quite rare, their distribution patterns are not as reliable as those for more abundant forms.

The lack of pronounced latitudinal gradients among mid-Cretaceous nannofloras is quite surprising. There are, however, some high-latitude species. The best pattern is shown by *Seribiscutum primitivum* (Fig. 13).

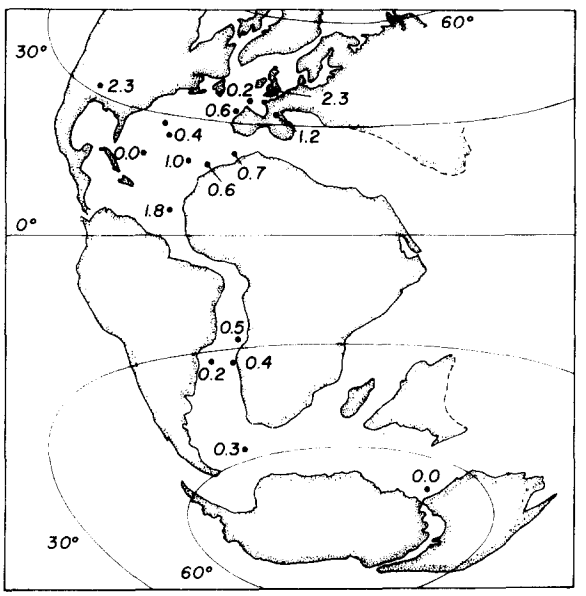

Fig. 11. Biogeographic distribution of the genus *Broinsonia* plotted as average relative abundance (%) at sites from the Atlantic, Indian oceans and adjacent seas, NC 10/11.

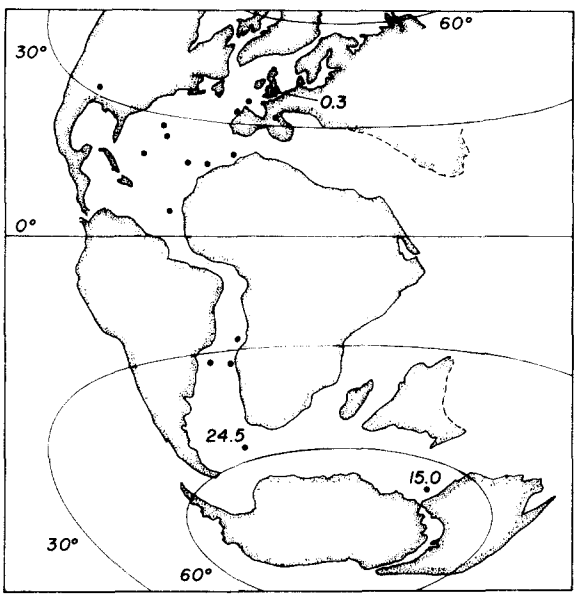

Fig. 13. Biogeographic distribution of *Seribiscutum primitivum*, plotted as average relative abundance (%) at sites from the Atlantic, Indian oceans and adjacent seas, NC 10/11.

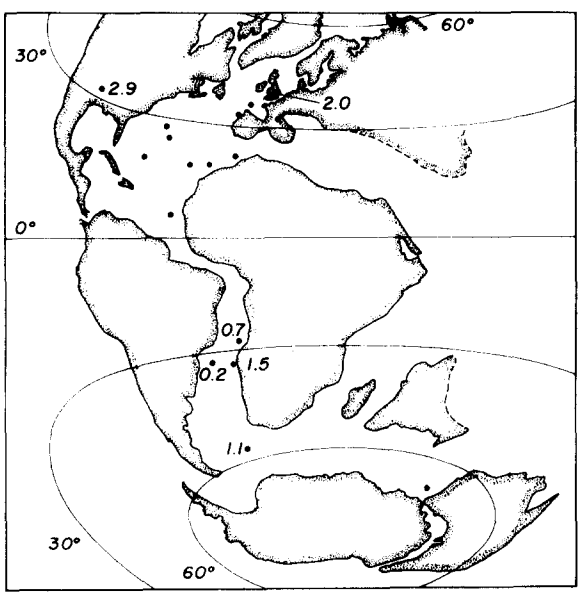

Fig. 12. Biogeographic distribution of the genus *Nannoconus*, plotted as average relative abundance (%) at sites from the Atlantic, Indian oceans and adjacent seas, NC 10/11.

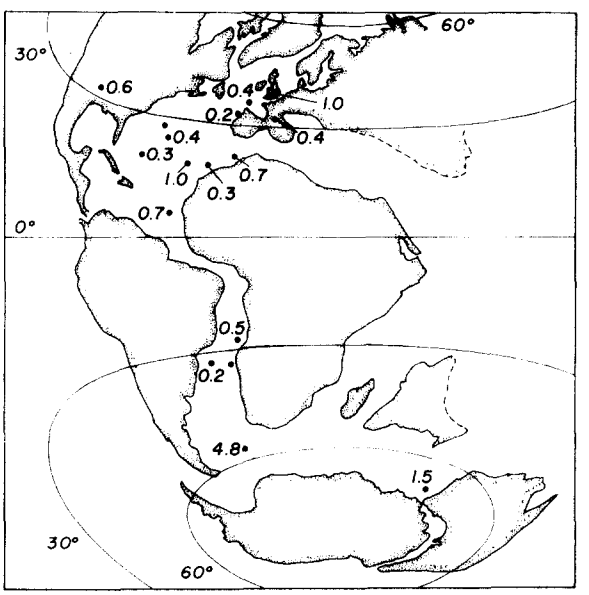

Fig. 14. Biogeographic distribution of *Lithastrinus floralis*, plotted as average relative abundance (%) at sites from the Atlantic, Indian oceans and adjacent seas, NC 10/11.

It is most abundant on the Falkland Plateau (Site 327) and at Site 258 off the west coast of Australia. It is present in the Cenomanian chalks of England and the North Sea (unpublished observations), the Cenomanian of the Normandy Coast (Amedro et al., 1978), the type Albian of the Paris Basin (Manivit, 1979) and the Cenomanian of Utah and Wyoming (unpublished observations). *Seribiscutum primitivum* is missing from low latitude sites. Thus, *Seribiscutum primitivum* is clearly a high latitude form. Another species that shows increased relative abundance at high latitudes is *Zygodiscus spiralis*; it is present at low latitude sites but it is much more abundant at high latitude sites (Sites 258, 327). Finally, *Lithastrinus floralis* (Fig. 14) also appears to be more abundant at high latitudes; its greatest average concentration was observed on the Falkland Plateau (Sites 327 and 330) and it shows consistently high relative abundances in the Indian Ocean off Australia (Site 258).

Other species that occur consistently do not show clear distribution patterns. An example of such a species is *Eiffellithus turriseiffeli* (Fig. 15). Neither latitudinal nor E—W trends can be discerned and we do not know any underlying paleoceanographic parameter that might explain the distribution pattern of this species. We show the distribution pattern here because it dominates one of the factors and it is an example of a major species that lacks pronounced biogeographic patterns in our data set.

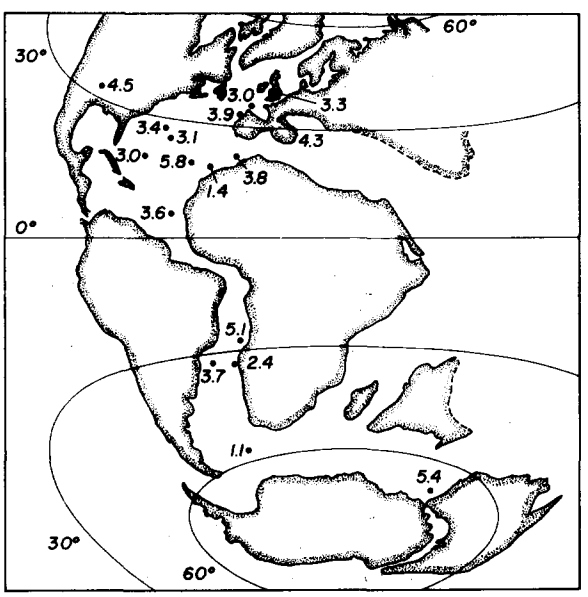

Fig. 15. Biogeographic distribution of *Eiffellithus turriseiffeli*, plotted as average relative abundance (%) at sites from the Atlantic, Indian oceans and adjacent seas, NC 10/11.

We proceed now to discuss the results of our multivariate statistical analysis. An *R*-mode factor analysis using relative abundances of eleven species for time slice NC 10/11 was performed; the following species or genera were included: *Rhagodiscus asper/R. splendens*, *Watznaueria barnesae*, *Lithraphidites carniolensis*, *Biscutum constans*, *Deflandrius cretaceus*, *Zygodiscus erectus*, *Lithastrinus floralis*, *Seribiscutum primitivum*, *Eiffellithus turriseiffeli*, *Broinsonia* spp. and *Nannoconus* spp. Four factors were extracted and a varimax rotation was performed on these factors. Table IX shows the factor loadings and scores. Factor scores at the various stations were printed out and plotted on Figs. 16—19. Factor 1 shows highest loadings for *Seribiscutum primitivum* and *Lithastrinus floralis* and scores highest at high southern latitudes (Fig. 16). It is a high latitude factor. Factor 2 has highest positive loadings for *Biscutum constans* and *Zygodiscus erectus* and highest negative loadings for *Watznaueria barnesae*; it is interpreted as a surface-water fertility factor. Highest positive factor scores are found along the eastern margin of the North Atlantic, highest negative scores in the western North Atlantic and in the South Atlantic (Fig. 17).

Factor 3 has the highest loadings for *Broinsonia* and *Nannoconus* and highest scores for this factor are found in Texas and the chalk of England (Fig. 18). This is a neritic factor with a fairly restricted distribution.

The last factor, Factor 4, shows highest loadings for *Eiffellithus turriseiffeli*. The highest scores for this factor are found at

TABLE IX

Varimax rotated factor matrix, NC 10/11

Species	Factor loadings			
	1	2	3	4
W. barnesae	0.01258	−0.90187	−0.05850	−0.02692
Z. erectus	−0.16566	0.74876	−0.21680	−0.46430
B. constans	0.00431	0.78659	0.04315	0.31870
S. primitivum	0.94678	−0.26174	−0.12749	−0.13668
L. floralis	0.90784	−0.21526	0.08290	−0.16256
Broinsonia	−0.00391	0.26875	0.89267	0.17497
Nannoconus	0.04421	−0.21280	0.82187	−0.05087
L. carniolensis	−0.59955	0.27989	−0.25338	−0.44243
E. turriseiffeli	−0.09604	0.12654	0.02672	0.93035
D. cretaceus	0.58250	0.31129	0.07774	0.26801
R. asper + splend.	−0.53984	−0.31126	−0.02088	−0.00077
Site	**Factor scores**			
105	−0.867107	−0.776771	−0.810943	−0.171354
137	−0.337993	0.817180	−0.063093	1.886499
258	1.887635	−0.049260	−1.148393	1.415967
327	3.030401	−1.116119	0.114251	−1.469249
356	−0.696731	−0.969334	−0.432690	0.138346
363	−1.733722	−0.680421	0.164447	−0.910192
364	−0.332290	0.000616	−0.443713	0.883388
367	0.588467	1.268332	0.716191	0.296262
369	−0.015713	2.151768	−0.501176	−2.098932
370	−0.588332	0.793734	−0.493281	0.148788
386	−1.078059	−1.179657	−0.394807	−0.027014
398	0.371797	1.088626	−0.302613	−0.015229
400	−0.715707	0.002575	−0.704359	−0.542696
418	0.270901	−0.666621	−0.658546	−0.301235
Bar	−0.267132	−0.817983	2.094084	−0.121296
Fr	0.367006	−0.440823	0.520837	0.420036
Tex	0.136587	0.554160	2.343703	0.467912

Site 137 in the North Atlantic and at Site 258 off the west coast of Australia (Fig. 19). It is difficult to see what these two locations have in common. Also, a highly negative score at Site 327 on the Falkland Plateau (Fig. 19) indicates that high latitude is not important in producing high scores for Factor 4. We do not have a good environmental explanation for the factor score pattern for this Factor 4 nor do we know what environmental pattern would be associated with the distribution pattern of the species with the highest loadings on this factor, *E. turriseiffeli*. This Factor 4 explains about 14% of the variance and is thus not trivial. If we now return to the principal components and their loadings that were obtained before varimax rotation we gain a little insight into the relationship of *E. turriseiffeli* with other species.

Principal component analysis also results in four significant principal components with eigenvalues larger than one (Table X). The first principal component shows highest positive loadings for *Seribiscutum primitivum* and *Lithastrinus floralis*, the two high-latitude forms. The second principal component has

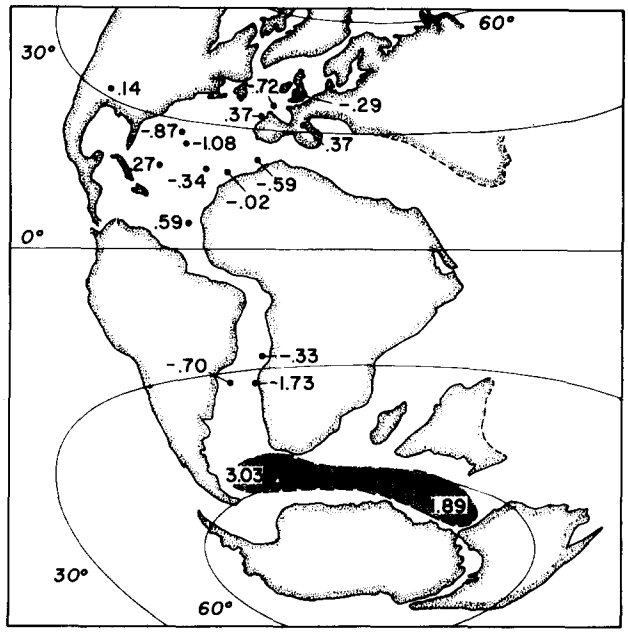

Fig. 16. Biogeographic distribution of factor scores for Factor 1, NC 10/11.

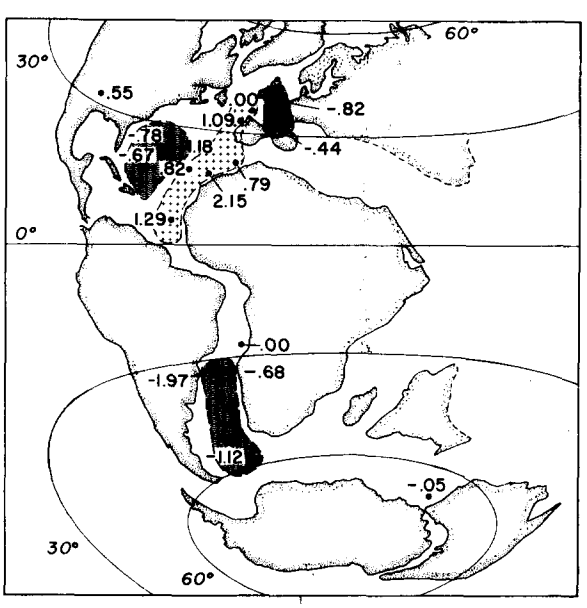

Area of high positive scores

Area of high negative scores

Fig. 17. Biogeographic distribution of factor scores for Factor 2, NC 10/11.

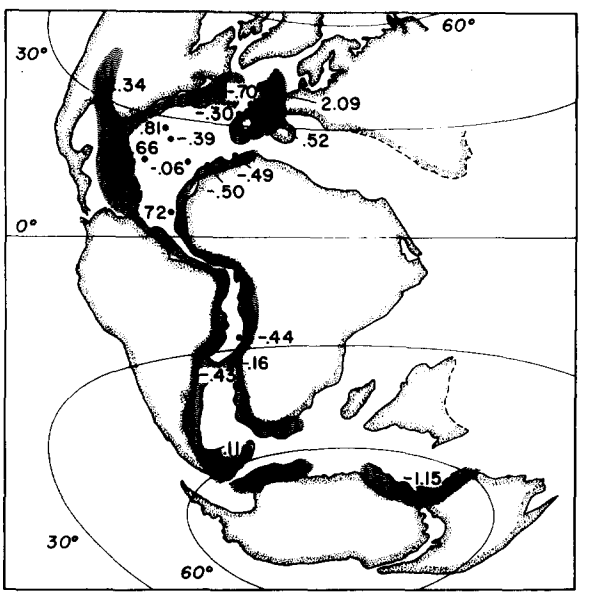

Fig. 18. Biogeographic distribution of factor scores for Factor 3, NC 10/11.

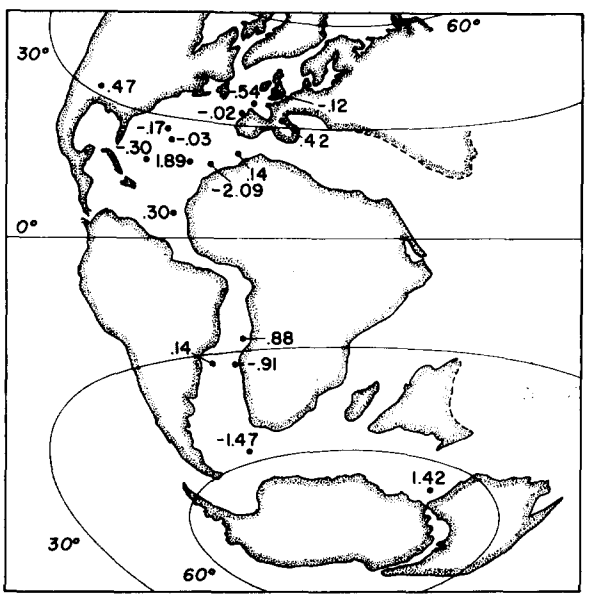

Fig. 19. Biogeographic distribution of factor scores for Factor 4, NC 10/11.

highest positive loadings for *Biscutum constans* and high negative loadings for *Watznaueria barnesae*. It does not load heavily on *Zygodiscus erectus*. The third principal component loads heavily on *Broinsonia* and

TABLE X

Principal component analysis with iterations NC 10/11

Species	Principal components loadings			
	1	2	3	4
W. barnesae	0.51896	−0.70201	0.21085	−0.10534
Z. erectus	−0.62015	0.25845	−0.56814	0.27658
B. constans	−0.42551	0.72266	−0.03048	−0.13394
S. primitivum	0.88540	0.15469	−0.43811	−0.00555
L. floralis	0.85632	0.22456	−0.30919	0.15650
Broinsonia	−0.01950	0.52711	0.62396	0.48185
Nannoconus	0.27371	0.08413	0.57641	0.55772
L. carniolensis	−0.70313	−0.29964	−0.27810	0.19033
E. turriseiffeli	−0.09578	0.39180	0.53439	−0.66578
D. cretaceus	0.31463	0.62386	−0.10898	−0.11638
R. asper + splend.	−0.25169	−0.47934	0.30879	−0.01650

Nannoconus; *Eiffellithus turriseiffeli* has a score that is just slightly lower than the one for *Nannoconus*. Thus, *E. turriseiffeli* appears to group with the neritic forms. The relationship is not very strong because *E. turriseiffeli* shows a high negative loading on principal component 4 but loadings for *Nannoconus* and *Broinsonia* are positive in principal component 4. The correlation coefficient matrix (Table XI) shows the highest correlation of *E. turriseiffeli* with *Biscutum constans* which is higher than the correlation coefficient of *B. constans* and *Zygodiscus erectus*. This could be seen as an indication of preference for nutrient rich waters for *E. turriseiffeli*. An *R*-mode cluster analysis restricted to the best preserved samples from the Atlantic (unpublished data) also grouped *E. turriseiffeli* with *Broinsonia*, giving some support for the speculation that it prefers neritic settings. Thus, neritic conditions, high fertility and good preservation appear to result in high relative abundance of *E. turriseiffeli*. Thus, considering other statistical data the distribution pattern of *E. turriseiffeli* we feel it preferred fairly nutrient-rich neritic conditions but we do not fully understand the parameters that controlled its distribution. The fact that we cannot explain the factor score patterns for Factor 4 is not just due to our inability to separate the contributions of common and unique variance because communality for *E. turriseiffeli* is high (0.89).

Thus, three of the four factors can be related to possible paleoenvironmental conditions, namely surface-water fertility for Factor 1, neritic conditions for Factor 2 and high latitude for Factor 3. A complete explanation for the last factor remains somewhat elusive and perhaps more data would provide more insight into possible parameters controlling the distribution of this factor.

An inspection of the communalities of species variables (Table XII) also shows that we have probably identified all the species that have high common variances. This confirms initial studies on the biogeographic distribution patterns of the more abundant middle Cretaceous nannofossil species by Roth and Bowdler (1981) and Roth (1981). In the former study *Rhagodiscus splendens* did show a similar pattern to *Watznaueria barnesae* for time slice NC 10/11 but no clear pattern for time slice NC 8. Dissolution could explain a similar pattern for the two species during NC 10/11 time. Other species plotted by Bowdler (1978) lacked clear biogeographic patterns and were thus not published by Roth and Bowdler (1981).

TABLE XI

Correlation coefficients, NC 10/11

	W. barnesae	*Z. erectus*	*B. constans*	*S. primitivum*	*L. floralis*	*Broinsonia*	*Nannoconus*	*L. carniolensis*	*E. turriseiffeli*	*D. cretaceus*	*R. asper + splend.*
W. barnesae	1.00000	–0.66676	0.74937	0.24042	0.20670	–0.26964	0.12032	–0.22985	–0.12158	–0.37416	0.14128
Z. erectus	–0.66676	1.00000	0.37167	–0.28732	–0.29794	–0.04549	–0.36670	0.52523	–0.36480	0.05149	–0.15411
B. constans	–0.74937	0.37167	1.00000	–0.26317	–0.15406	0.28989	–0.12023	0.13478	0.44860	0.19096	–0.39055
S. primitivum	0.24042	–0.28732	–0.26317	1.00000	0.91612	–0.26119	0.05322	–0.52275	–0.24499	0.42657	–0.49724
L. floralis	0.20670	–0.29794	–0.15406	0.91612	1.00000	–0.02844	0.16304	–0.56994	–0.29455	0.36102	–0.47321
Broinsonia	0.26964	–0.04549	0.28989	–0.26119	–0.02844	1.00000	0.65870	–0.26945	0.19389	0.25839	–0.06083
Nannoconus	0.12032	–0.36670	–0.12023	0.05322	0.16304	0.65870	1.00000	–0.21030	–0.02276	–0.08129	0.00185
L. carniolensis	–0.22985	0.52523	0.13478	–0.52275	–0.56994	–0.26945	–0.21030	1.00000	–0.30609	–0.54647	–0.08260
E. turriseiffeli	–0.12158	–0.36480	0.44860	–0.24499	–0.29455	0.19389	–0.02276	–0.30609	1.00000	0.20640	–0.05704
D. cretaceus	–0.37416	0.05149	0.19096	0.42657	0.36102	0.25839	–0.08129	–0.54647	0.20640	1.00000	–0.34571
R. asper + splend.	0.14128	–0.15411	–0.39055	–0.49724	–0.47321	–0.06083	–0.00185	0.08260	–0.05704	–0.34571	1.00000

TABLE XII

Factor analysis, NC 10/11

Variable	Communality	Factor	Eigenvalue	Variance (%)	Cum. (%)
W. barnesae	0.81768	1	3.09338	36.8	36.8
Z. erectus	0.85066	2	2.30338	27.4	64.2
B. constans	0.72218	3	1.84741	22.0	86.1
S. primitivum	0.99983	4	1.16705	13.9	100.0
L. floralis	0.90381				
Broinsonia	0.89972				
Nannoconus	0.72529				
L. carniolensis	0.69774				
E. turriseiffeli	0.89150				
D. cretaceus	0.51408				
R. asper + splend.	0.38874				

Time slice NC 8/9

Biogeographic distribution patterns of important Atlantic nannofossils in the Atlantic for this middle Albian time slice appear to be similar to the ones for the time slice NC 10/11 (Roth and Bowdler, 1981). Preservation of calcareous nannofossils is generally poorer in time slice NC 8/9 than in time slice NC 10/11. A factor analysis excluding *Watznaueria barnesae* was performed to test the effect of the exclusion of the dominant species which could effect the abundance of all other species when its abundance fluctuations are large (closure problem). The resulting overall distribution patterns were largely similar to the ones including *W. barnesae* and are thus not presented. This second analysis did show, however, that the closure problem is not serious.

In the factor analysis all species of *Watznaueria* (i.e., *W. barnesae*, *W. communis*, *W. biporta* and *W. britannica*) are combined and included as *Watznaueria* spp. Other species and genera included in this analysis are *Rhagodiscus asper/R. splendens* (combined), *Braarudosphaera* spp., *Biscutum constans*, *Zygodiscus erectus*, *Zygodiscus* spp. (includes *Z. erectus*, *Z. elegans*, *Z. diplogrammus*

TABLE XIII

Principal component analysis with iterations, NC 8/9

Species	Principal component loadings		
	1	2	3
A. asper + splend.	0.00377	0.99388	−0.03178
Braarudosphaera	−0.04739	0.11111	0.78743
B. constans	0.76453	−0.24153	0.41438
Z. erectus	0.89638	0.25718	−0.29289
Watznaueria spp.	−0.78185	−0.14172	−0.04245
Zygodiscus spp.	0.78367	0.29869	−0.47093
S. primitivum	−0.31570	−0.47106	−0.15771
Site	**Principal component scores**		
258	−1.163696	−1.628818	−0.836393
259	−1.082819	−2.307698	0.181546
327	−0.210833	−0.284879	0.954788
330	−0.588332	−1.248473	1.565530
363	−0.651071	0.681479	1.810613
364	0.989169	1.449300	−0.028830
369	2.916707	−0.802064	−0.243641
370	0.235192	0.785924	−1.211907
386	0.151050	0.631446	−1.050453
390	0.650376	−0.059454	0.349326
391	−0.330558	−0.103012	−0.004536
392	1.508775	0.739583	1.196596
398	1.048930	−0.822340	−0.734338
400	−0.111029	−0.300502	−0.131144
402	−0.215808	0.254170	−0.797854
418	−0.429774	1.194656	0.127437
France	−0.674619	0.856238	−0.443237
Gault	0.041656	0.073521	−1.329294
Texas	−0.021664	0.890926	0.625499

and *Z. spiralis*) and finally *Serbiscutum primitivum*.

Three factors with eigenvalues exceeding 1.0 were extracted from the data matrix (Table XIII). Factor 1 has highest positive loadings for *Zygodiscus erectus*, *Biscutum constans* and *Zygodiscus* spp. *Watznaueria* spp. shows a high negative loading on Factor 1. High positive factor scores for Factor 1 occur at Sites 369 and 398 in the eastern North Atlantic; the high positive score for Factor 1 at Site 392 is somewhat unexpected. High negative loadings were observed in the poorly preserved samples from the Indian Ocean (Sites 258 and 259) and the South Atlantic (Sites 363, 364) and in the western North Atlantic (Sites 391 and 418; Fig. 20). We interpret this factor 1 as a fertility factor. High positive scores appear to occur on the eastern margins of the Atlantic where upwelling conditions existed. The highly positive score at Site 392 (Fig. 20) due to great abundance of *Z. erectus* (see also Roth and Bowdler, 1981, fig.15), appears to be due to the existence of fairly nutrient-rich waters at this shallow site.

Factor 2 shows highest positive loading for *Rhagodiscus asper/R. splendens* and highest negative loading for *Seribiscutum primitivum* (Table XIII). As shown by Roth and Bowdler (1981) *R. asper/R. splendens* do not show clearly defined patterns for time-slice NC 8/9; some preference for oceanic settings and possibly a slight preference for lower latitudes are supported by the results of this factor analysis. Highest positive scores for Factor 2 occur at Sites 364 and 418, followed by Sites 370, 392, 363 and 386. Moderately high positive scores also occur at the two epicontinental sections in southeastern France and Texas. Highly negative scores caused by high negative loadings for *Seribiscutum primitivum* are found at the high latitude sites on Falkland Plateau and in the Indian Ocean (Fig. 21). Thus, Factor 2 appears to be a high latitude/low latitude factor, although the exact ecologic preference of *R. asper/R. splendens* remains elusive.

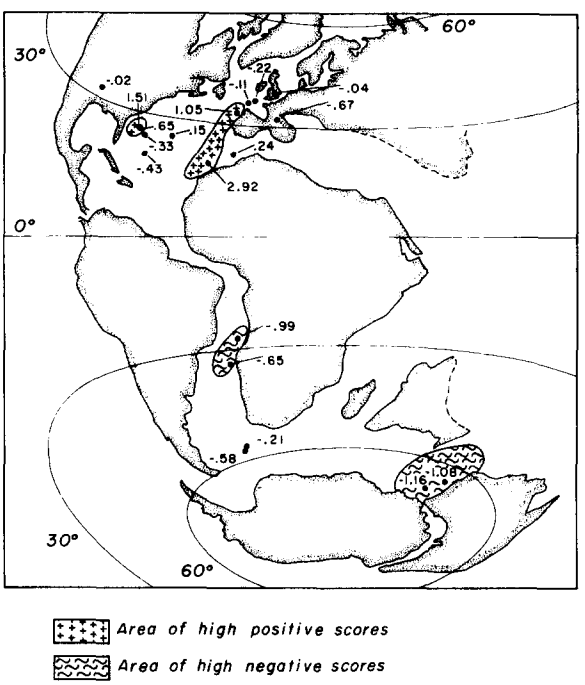

Fig. 20. Biogeographic distribution of factor scores for Factor 1, NC 8/9.

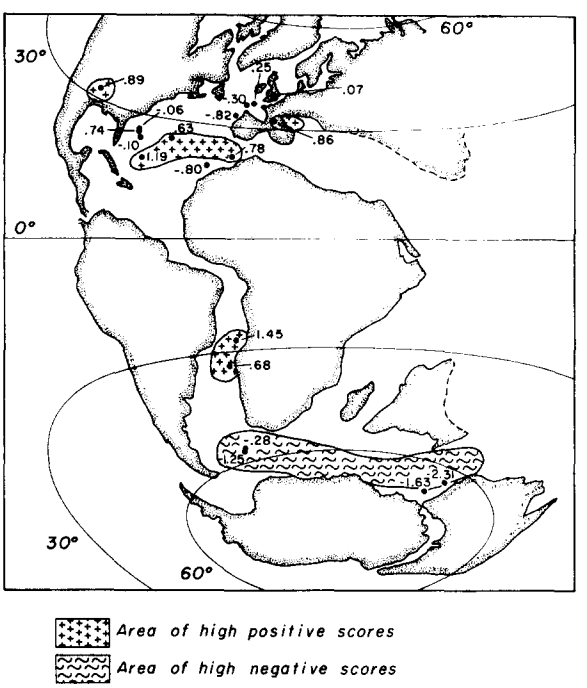

Fig. 21. Biogeographic distribution of factor scores for Factor 2, NC 8/9.

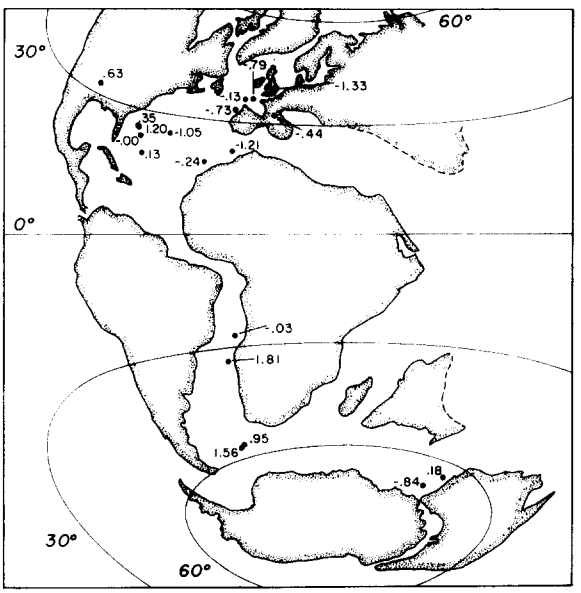

Fig. 22. Biogeographic distribution of factor scores for Factor 3, NC 8/9.

Factor 3 shows highest positive loadings on *Braarudosphaera* spp. and *Biscutum constans* and highest negative loadings on *Zygodiscus* spp. (Table XIII). Highest positive scores are found in samples from shallow plateau locations (Sites 363, 327 and 392). High negative loadings are from samples rich in *Zygodiscus* spp., indicative of nutrient-rich waters, such as Site 370 and the epicontinental Gault Clay (Fig. 22). Thus, Factor 3 shows neritic effects.

The results of this factor analysis does show the major trends in nannofossil biogeography established for time slice NC 10/11, i.e., a distinction of high fertility, high latitude and neritic assemblages.

Time slice NC 7

Our data set for the late Aptian to early Albian or middle Magellanian time slice NC 7 only includes samples from the Atlantic because none of the DSDP Sites in the Indian Ocean recovered sediments of this age that contain nannofossils. An *R*-mode factor analysis was performed using species percentages in the best preserved samples from 14 locations rather than average abundances derived from many samples because of a paucity of data. The following twelve species were included in the factor analysis: *Rhagodiscus asper/R. splendens*; *Zygodiscus elegans*; *Z. erectus*; *Z. diplogrammus*; *Z. spiralis*; *Watznaueria barnesae*; *Lithraphidites carniolensis*; *Braarudosphaera* spp.; *Biscutum constans*; *Broinsonia* spp.; *Nannoconus* spp.; and *Vagalapilla* spp. Four factors with eigenvalues of more than 1.0 were extracted (Table XIV).

Factor 1 loads heavily on *Zygodiscus diplogrammus*, *Z. elegans* and *Vagalapilla* spp. Its highest scores are found at Site 370 (Fig. 23). We interpret this factor as an indicator of high surface-water fertility.

Factor 2 is dominated by *Zygodiscus spiralis*, *Biscutum constans* and *Zygodiscus erectus*. It scores highest at Sites 402 and 400 in the eastern North Atlantic and shows similar scores at Site 418 (Fig. 24). We consider it a fertility indicator, possibly with some preference for high latitudes.

Factor 3 is a neritic factor with high loadings on *Braarudosphaera* spp. and *Nannoconus* spp. Highest scores for this factor occur at the shallow margin Sites 392, 402 and 390 (Fig. 25). *Nannoconus* spp. and *Braarudosphaera* spp. do not occur in our Gault Clay sample from England despite its neritic setting. Samples from southern France show positive scores and thus neritic influences for that region.

Factor 4 weighs most heavily on *Broinsonia* spp. and *Rhagodiscus asper/R. splendens*. Its highest score occurs at Site 327 on the Falkland Plateau followed by Site 364 in the Angola Basin; a high negative score is found in the Gault Clay of England (Fig. 26). It is difficult to interpret the paleoceanographic implications of this factor. It is probably indicative of poor preservation and neritic effects. A low but positive loading for this factor at Site 361 could be explained by downslope transport of sediment initially deposited at shallower depth.

TABLE XIV

Factor analysis with varimax rotation, NC 7

Species	Factor loadings			
	1	2	3	4
R. asper + splend.	−0.02132	−0.02306	0.08249	0.73794
Z. spirali	−0.10323	0.75650	−0.24763	0.51590
W. barnesae	−0.45619	−0.61041	−0.62678	−0.15763
L. carniolensis	0.11584	0.56116	0.36369	−0.19669
Braarudosphaera	−0.02606	−0.11687	0.93466	−0.01806
B. constans	−0.00066	0.70119	−0.04239	0.04251
Broinsonia	0.03722	−0.00930	−0.18245	0.93407
Z. diplogrammus	0.90641	0.20853	−0.03785	−0.15189
Z. elegans	0.89000	0.11772	−0.10338	−0.10576
Nannoconus	−0.15246	0.00369	0.83828	−0.08177
Z. erectus	0.35236	0.66532	−0.09397	−0.25512
Vagalapilla	0.73632	−0.05677	0.03271	0.22362
Site	Factor scores			
327	0.129304	−0.032309	−0.633908	3.245318
361	−0.848899	−1.324404	−0.072675	0.406851
370	2.878683	−0.364465	−0.452565	−0.543379
390	0.517903	0.917454	0.783755	−0.442457
391	0.355911	−0.273673	0.510102	−0.004320
400	−0.404296	1.309710	−0.567387	0.101815
398	0.324403	0.740370	−0.370301	−0.178455
402	−0.749604	2.774563	1.025422	−1.107136
392	−0.290335	2.823715	2.549351	0.929835
364	−0.929544	−0.249350	−0.459497	−0.448493
Gault	−1.107101	−1.542204	−2.440079	−1.546661
Fr 69	0.478532	0.220525	0.553593	−0.020676
Fr 70	0.038760	−1.193271	0.005901	0.106628
418	−0.393721	1.840775	−0.431724	−0.498882

In summary, we recognized two factors indicative of surface water fertility for time slice NC 7. A clear high latitude assemblage is difficult to identify although a combined fertility/high latitude factor appear to exist. One neritic factor appears to be clearly identifiable in the present data set.

Factor analyses performed for the three time slices allowed us to reduce the redundancy of information contained in the distribution patterns of individual nannofossil species and group various species into smaller, more manageable variables (factors) that can be related more easily to paleoceanographic parameters. For time slice NC 10/11 a high latitude factor with *Seribiscutum primitivum* and *Lithastrinus floralis* shows highest scores at high southern latitudes. The high productivity factor (with highest loadings for *Biscutum constans* and *Zygodiscus erectus*) dominates along the eastern margin of the North Atlantic and in the South Atlantic. A neritic factor with high loadings for *Broinsonia* and *Nannoconus* is found in Texas and the chalk of England.

A high latitude factor, a high productivity and a neritic factor were also extracted for time-slice NC 8/9. For time-slice NC 7 one high latitude factor, two high productivity factors and two neritic factors were extracted.

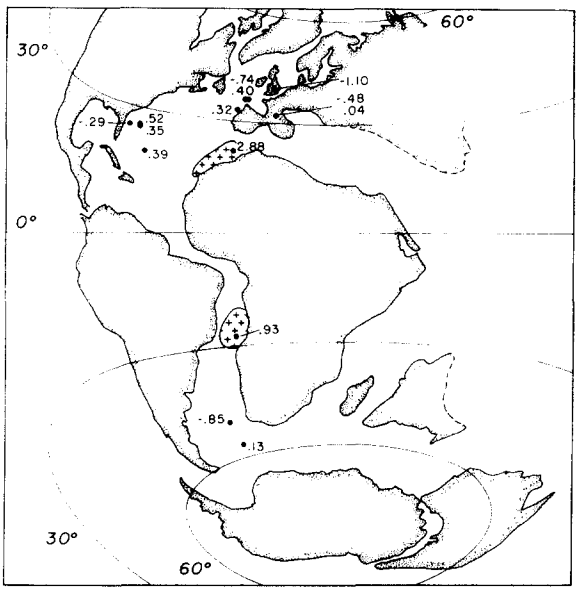

Area of high positive scores

Fig. 23. Biogeographic distribution of factor scores for Factor 1, NC 7.

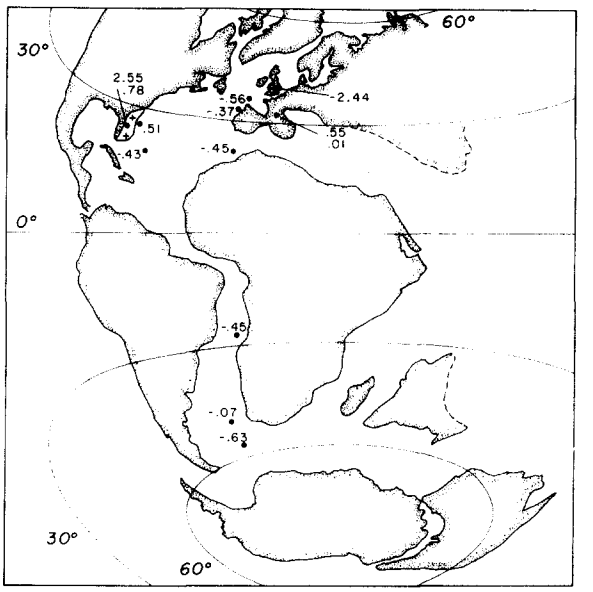

Area of high positive scores

Fig. 25. Biogeographic distribution of factor scores for Factor 3, NC 7.

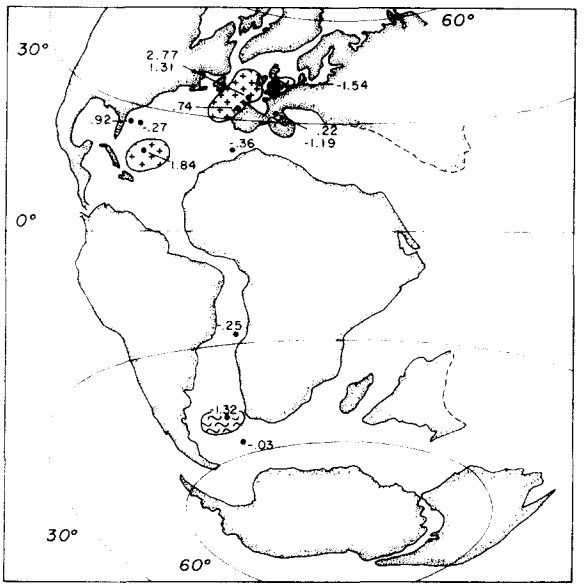

Area of high positive scores

Area of high negative scores

Fig. 24. Biogeographic distribution of factor scores for Factor 2, NC 7.

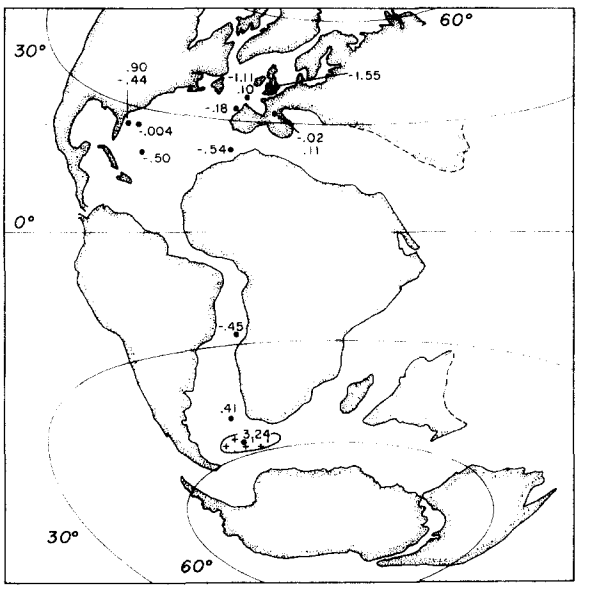

Fig. 26. Biogeographic distribution of factor scores for Factor 4, NC 7.

East—west surface water fertility gradients were less pronounced during this oldest time slice and latitudinal nannofloral trends were even less pronounced than in the two younger time slices.

Factor analysis thus provides considerable insight into biogeographic patterns and facilitated their paleoceanographic interpretation. High latitude, high fertility and neritic factors with reasonably clear biogeographic distribution patterns were extracted from all three time slices.

Discussion of biogeography

Biogeographic patterns of calcareous nannofossils are most clearly defined in the upper Albian to Cenomanian (NC 10/11 time slice). Cool water assemblages are largely restricted to high southern latitudes (S of 50°) in the South Atlantic and the Indian oceans, with only a small component of such high latitude species in England and France. This is indicative of a wide tropical—subtropical zone where nannofossil distribution is fairly homogeneous.

The biogeographic distribution of these tropical to subtropical nannofossil assemblages appears to be largely controlled by surface water fertility. We notice a clear E—W trend in the distribution of nannofossil assemblages in the North Atlantic. High fertility ("upwelling") assemblages are dominant along the eastern margin of the Atlantic and oceanic assemblages occur in the central and western North Atlantic. This appears to agree with the distribution of organic matter in the sediments. Broadly speaking, organic matter of marine origin is largely restricted to the eastern North Atlantic and organic matter of terrestrial origin occurs in the western Atlantic (Tissot et al., 1979, 1980). Epicontinental sea deposits and some continental margin sediments contain neritic assemblages and probably reflect more variable paleoceanographic conditions, i.e., fluctuating salinity, temperature and nutrient supply.

Biogeographic distribution patterns of calcareous nannofossils during the middle Albian (time slice NC 8/9) are similar to those of the late Albian/Cenomanian (time slice NC 10/11). We still find high latitude assemblages in the South Atlantic and Indian oceans. High fertility assemblages also occur along the eastern margin of the North Atlantic and are also observed on the Blake Nose in the western Atlantic. A single middle Albian horizon rich in organic matter of marine origin reported from Site 390 on the Blake Nose (Tissot et al., 1980) lends support to our speculation that waters along the western margin of the Atlantic were periodically enriched in nutrients, possibly caused by zonal upwelling (Parrish, 1982; Parrish et al., 1982). Neritic assemblages are also observed in middle Albian sediments from shallow sites and epicontinental seas.

Only samples from the Atlantic Ocean were available for the early Albian to late Aptian (time slice NC 7). Once again high fertility and oceanic assemblages can be recognized. Neritic assemblages also occur at continental margin locations. High-latitude assemblages are difficult to recognize because of the lack of a good marker species.

What can we learn from the biogeographic patterns of nannofossils in the Atlantic and Indian oceans during the late Aptian to early Cenomanian? Preservational changes have affected nannofossil assemblages but original paleoceanographic signals are still recorded. Surface-water temperature gradients appear to have been low during the middle Cretaceous. Cool- to temperate-water assemblages are restricted to fairly high latitudes and low-latitude assemblages are largely controlled by fertility. Thus, a wide tropical to subtropical zone existed during the middle Cretaceous. Meridional upwelling occurred along the eastern margin of the North Atlantic and we may have had zonal upwelling extending to the western margin of the North Atlantic, especially during the middle Albian. Variable oceanographic conditions existed in epiconti-

nental seas and the shallowest parts of the Atlantic, especially over plateaus (Falkland Plateau) and ridges (Rio Grande Rise—Walvis Ridge). Blooms of individual species occurred in the South Atlantic and indicate restricted sea conditions with upwelling caused by obstacles to intermediate currents such as the Falkland Plateau and Rio Grande—Walvis Ridge (Roth and Bowdler, 1981).

Conclusions

In spite of a limited data base and relatively poor preservation, nannofossil preservation and biogeography put some constraints on climatic and paleoceanographic models for the middle Cretaceous. With our new nannofossil data, some theoretical considerations (Barron and Washington, 1982; Lloyd, 1982; Parrish and Curtis, 1982; Barron, 1983) and a liberal amount of imagination we attempt to reconstruct surface and deep circulation (Figs. 27 and 28). A strong westward current dominated in the Tethys, it is an extension of the Pacific North Equatorial Current deflected by the Horn of Africa. In the North Atlantic a clockwise gyre developed. Current patterns in the southern Indian Ocean are much more speculative.

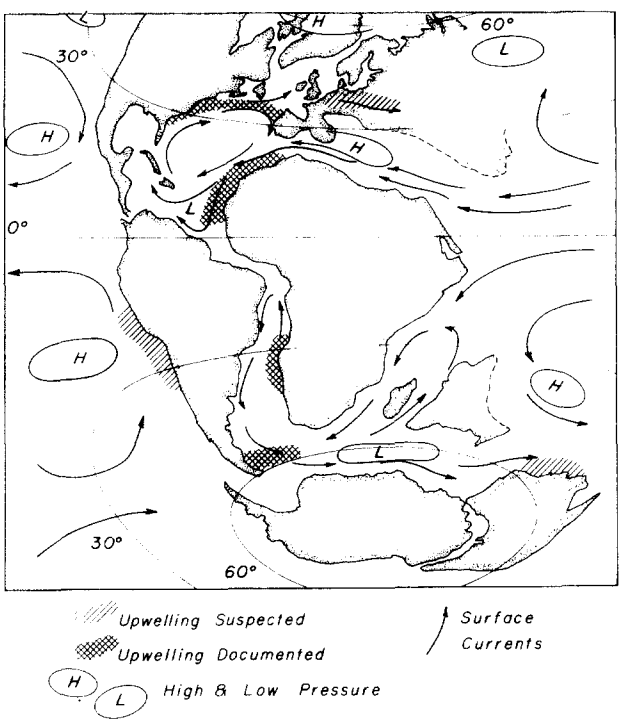

Fig. 27. Surface water circulation, upwelling areas and atmospheric pressure distribution in the mid-Cretaceous Atlantic and Indian oceans.

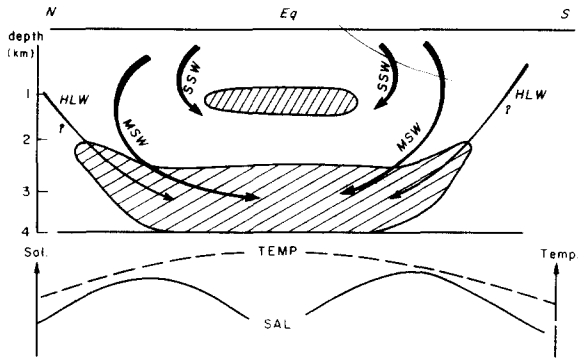

Fig. 28. Intermediate and deep water circulation and temperature/salinity profile in the mid-Cretaceous Atlantic Ocean. Hatchured areas indicate low dissolved oxygen concentrations. (Abbreviations: *SSW* = salty surface water; *MSW* = marginal seas salty water; *HLW* = high latitude water; *Sal* = salinity; *Temp* = temperature.)

Meridional (coastal) upwelling has been documented for the northwestern coast of Africa and less clearly for the South Atlantic off the west coast of Southern Africa. Zonal upwelling is postulated for the northern North Atlantic (extending to the Blake Nose during the late Aptian to middle Albian but only documented off the coast of Spain during time slice NC 10/11). Zonal upwelling, combined with forcing of intermediate water over the shallow plateau, occurred over the Falkland Plateau where monospecific blooms of nannofossils were observed (Noël and Manivit, 1978; Roth and Bowdler, 1981).

Upwelling conditions along the west coast of Australia postulated by Parrish and Curtis (1982) did not extend to the location of Sites 258 and 259 and could not be documented by the scarce nannofossil data for this ocean. Other upwelling regions are inferred from the atmospheric circulation patterns (Barron and

Washington, 1982; Parrish and Curtis, 1982) but nannofossil data are unavailable to substantiate their existence.

Much speculation about the chemistry and circulation of deep and intermediate water and its effect on black shale formation has been published. Such models include: (1) density stratification because of a fresh water lid analogous to the conditions present during Quaternary sapropel formation in the Mediterranean (Ryan and Cita, 1977); (2) a more extensive oxygen minimum zone (Schlanger and Jenkyns, 1976); (3) high-density saline bottom waters derived from shallow marginal basins (Roth, 1976, 1978; Thierstein and Berger, 1978; Brass et al., 1982a); (4) spilling of oxygen depleted shelf waters (Jenkyns, 1980); and (5) warm waters of low initial oxygen content that became depleted in oxygen even under conditions of low biological productivity of surface water (Berger, 1979). Taking the preservational and biogeographic distribution patterns of calcareous nannofossils into account, we still favor a predominantly haline-driven deep circulation with marginal seas and subtropical high salinity waters as bottom water source (Fig. 28). Mixing of high saline subtropical waters with colder high latitude waters could have produced the densest waters (Wilde and Berry, 1982). We postulate the existence of oxygen poor highly saline bottom waters and a second mid-water oxygen minimum zone due to depletion of saline intermediate waters by falling organic matter.

Nannofossil preservational patterns thus lend some support to the circulation model of Wilde and Berry (1982) where saline deep waters and a widespread intermediate water oxygen minimum are postulated.

In summary, our observations of nannofossil distribution patterns support general climatic reconstructions for Cretaceous climates that indicate a more equable climate (Barron and Washington, 1982). The distribution of nannofossil assemblages indicative of upwelling conditions agrees well with information from organic geochemistry (Tissot et al., 1980) and the models of upwelling conditions by Parrish and Curtis (1982). All major areas of upwelling postulated on theoretical grounds in the latter paper also contain calcareous nannofossil assemblages indicative of upwelling conditions. Preservation of calcareous nannofossils is consistent with the warm saline bottom water hypothesis (Roth, 1978; Brass et al., 1982b) and the circulation model of Wilde and Berry (1982). Thus, calcareous nannofossil preservation and biogeographic distribution has allowed us to put some constraints on paleoceanographic and paleoclimatic models.

Acknowledgements

The earlier phases of this study were supported by NSF Grant OCE 76-21561. We thank J.L. Bowdler for some census data used in this study. Discussions with W.H. Berger, C. Summerhayes and H.R. Thierstein have been helpful. We are grateful to Angela Gorman for doing carbon analyses for us and performing some of the multivariate statistical analyses. We thank H.R. Thierstein for his careful review and Kadir Uygur for careful editing of this paper.

References

Amedro, F., Damotte, R., Manivit, H., Robaszynski, F. and Sornay, J., 1978. Échelles biostratigraphiques dans le Cénomanien du Boulonnais (macro—micro—nanno fossiles). Géol. Méditerr., 5(1): 5—18.

Barker, P.F., Dalziel, I.W.D. et al., 1977. Initial Reports of the Deep Sea Drilling Project, 36. U.S. Government Printing Office, Washington, D.C., 1080 pp.

Barron, E.J., 1983. A warm equable Cretaceous: the nature of the problem. Earth-Sci. Rev., 19: 305—338.

Barron, E.J. and Harrison, C.G., 1980. An analysis of past plate motions: The South Atlantic and Indian Oceans. In: P.A. Davies and S.K. Runcorn (Editors), Mechanisms of Continental Drift and Plate Tectonics. Academic Press, London, pp. 89—109.

Barron, E.J. and Washington, W.M., 1982. Cretaceous climate: A comparison of atmospheric simulations

with the geologic record. Palaeogeogr., Palaeoclimatol., Palaeoecol., 40: 103—133.

Barron, E.J., Thompson, S.L. and Schneider, S.H., 1981. An ice-free Cretaceous? Results from climate model simulations. Science, 212: 501—508.

Benson, W.E. and Sheridan, R.E. et al., 1978. Initial Reports of the Deep Sea Drilling Project, 44. U.S. Government Printing Office, Washington, D.C., 105 pp.

Berger, W.H., 1979. Impact of deep-sea drilling on paleoceanography. In: M. Talwani, W. Hay and W.B.F. Ryan (Editors), Deep Drilling Results in the Atlantic Ocean: Continental Margins and Paleoenvironments. Am. Geophys. Union, Washington, D.C., pp. 297—314.

Berger, W.H. and Winterer, E.L., 1974. Plate stratigraphy and the fluctuating carbonate line. Spec. Publ. Int. Assoc. Sedimentol., 1: 11—48.

Berner, R.A., 1971. Principles of Chemical Sedimentology. McGraw-Hill, New York, N.Y., 240 pp.

Bolli, H.M., Ryan, W.B.F. et al., 1978. Initial Report of the Deep Sea Drilling Project, 40. U.S. Government Printing Office, Washington, D.C., 1079 pp.

Bowdler, J.L., 1978. Mid-Cretaceous calcareous nannoplankton paleobiogeography and paleoceanography of the Atlantic Ocean. Thesis. Univ. Utah, Salt Lake City, 182 pp. (unpublished).

Brass, G.W., Saltzman, E., Sloan, J.L., Southam, J.R., Hay, W.W., Holser, W.T. and Peterson, W.H., 1982a. Ocean circulation, plate tectonics and climate. In: Climate in Earth History, Studies in Geophysics. Nat. Res. Counc. Nat. Acad. Press, Washington, D.C., pp. 83—89.

Brass, G.V., Southam, J.R. and Peterson, W.H., 1982b. Warm saline bottom water in the ancient ocean. Nature, 296: 620—623.

Davies, T.A. and Kidd, R.B., 1977. Sedimentation in the Indian Ocean through time. In: J.R. Heirtzler, H.M. Bolli, T.A. Davies, J.B. Saunders and J.G. Sclater (Editors), Indian Ocean Geology and Biostratigraphy. Am. Geophys. Union, Washington, D.C., pp. 61—85.

Davies, T.A., Luyendyk, B.P. et al., 1974. Initial Reports of the Deep Sea Drilling Project, 26. U.S. Government Printing Office, Washington, D.C., 1129 pp.

Dean, W.E. and Gardner, J.V., 1982. Origin and geochemistry of redox cycles of Jurassic to Eocene age, Cape Verde Basin (DSDP Site 307), continental margin of north-west Africa. In: S.O. Schlanger and M.B. Cita (Editors), Nature and Origin of Cretaceous Carbon-rich Facies. Academic Press, London, pp. 55—78.

Donnelly, T., Francheteau, J., Bryan, W., Robinson, P., Flower, M., Salisbury, M. et al., 1980. Initial Reports of the Deep Sea Drilling Project, 51—53. U.S. Government Printing Office, Washington, D.C., 1613 pp.

Frakes, L.A., 1979. Climates throughout Geologic Time. Elsevier, Amsterdam, 310 pp.

Habib, D., 1979. Sedimentary origin of North Atlantic Cretaceous palynofacies. In: M. Talwani, W. Hay and W.B.F. Ryan (Editors), Deep Drilling Results in the Atlantic Ocean: Continental Margins and Paleoenvironments. Am. Geophys. Union, Washington, D.C., pp. 420—437.

Habib, D., 1983. Sedimentation-rate-dependent distribution of organic matter in the North Atlantic Jurassic—Cretaceous. In: Initial Reports of the Deep Sea Drilling Project, 76. U.S. Government Printing Office, Washington, D.C., pp. 781—794.

Haq, B.U. and Lohmann, G.P., 1976. Early Cenozoic calcareous nannoplankton biogeography of the Atlantic Ocean. Mar. Micropaleontol., 1: 119—194.

Hayes, E.E., Pimm, A.C. et al., 1972. Initial Reports of the Deep Sea Drilling Project, 14. U.S. Government Printing Office, Washington, D.C., 975 pp.

Heath, G.R., Moore, T.C. and Dauphin, J.P., 1977. Organic carbon in deep-sea sediments. In: N.R. Anderson and A. Malahoff (Editors), The Fate of Fossil Fuel CO_2. Plenum Press, New York and London, 749 pp.

Hill, M.E., 1975. Selective dissolution of mid-Cretaceous (Cenomanian) calcareous nannofossils. Micropaleontology, 21: 227—235.

Hollister, C.D., Ewing, J.I. et al., 1972. Initial Reports of the Deep Sea Drilling Project, 11. U.S. Government Printing Office, Washington, D.C., 1077 pp.

Jenkyns, H.C., 1980. Cretaceous anoxic events: from continents to oceans. J. Geol. Soc. London, 137: 171—188.

Kagami, H., Ishizuka, T. and Aoki, S., 1983. Geochemistry and mineralogy of selected carbonaceous claystones in the lower Cretaceous from the Blake—Bahama Basin, North Atlantic. In: Initial Reports of the Deep Sea Drilling Project, 76. U.S. Government Printing Office, Washington, D.C., pp. 429—436.

Kelts, K. and Arthur, M.A., 1981. Turbidites after ten years of deep-sea drilling — wringing out the mop? Soc. Econ. Paleontol. Mineral. Spec. Pap., 32: 91—127.

Kemper, E., 1983. Ueber Kalt- und Warmzeiten der Unterkreide. Zitteliana, 10: 359—369.

Lancelot, Y., Seibold, E. et al., 1978. Initial Reports of the Deep Sea Drilling Project, 41. U.S. Government Printing Office, Washington, D.C., 1259 pp.

Lloyd, C.R., 1982. The mid-Cretaceous earth: Paleogeography, ocean circulation and temperature, atmospheric circulation. J. Geol., 90: 393—413.

Manivit, H., 1979. Le nannoplancton du stratotype

de l'Albien: biozonation, systématique, nannofaciès, paléoécologie. In: P. Rat (Editor), L'Albian de l'Aube. Les Stratotypes Français. C.N.R.S., Paris, pp. 307—340.

Nie, N.H., Hull, C.H., Jenkins, J.G., Steinbrenner, K. and Bent, D.H., 1975. SPSS: Statistical Package for the Social Sciences. McGraw-Hill, New York, N.Y., 675 pp.

Noël, D. and Manivit, H., 1978. Nannofaciès de "black shales" aptiennes et albiennes d'Atlantique sud (legs 36 et 40). Interêt sédimentologique. Bull. Soc. Géol. Fr., 20: 491—502.

Parrish, J.T., 1982. Upwelling and petroleum source beds with reference to Paleozoic. Am. Assoc. Pet. Geol. Bull., 66(6): 750—774.

Parrish, J.T. and Curtis, R.L., 1982. Atmospheric circulation, upwelling, and organic-rich rocks in the Mesozoic and Cenozoic eras. Palaeogeogr., Palaeoclimatol., Palaeoecol., 40: 31—66.

Parrish, J.T., Ziegler, A.M. and Scotese, C.R., 1982. Rainfall patterns and the distribution of coals and evaporites in the Mesozoic and Cenozoic. Palaeogeogr., Palaeoclimatol., Palaeoecol., 40: 67—101.

Roth, P.H., 1973. Calcareous nannofossils — Leg 17, Deep Sea Drilling Project. In: Initial Reports of the Deep Sea Drilling Project, 17. U.S. Government Printing Office, Washington, D.C., pp. 695—795.

Roth, P.H., 1976. Cretaceous calcareous nannofossil diversity and paleoceanography. Geol. Soc. Am. Abstr. Progr., 8(6): 1078.

Roth, P.H., 1978. Cretaceous nannoplankton biostratigraphy and oceanography of the northwestern Atlantic Ocean. In: Initial Reports of the Deep Sea Drilling Project, 44. U.S. Government Printing Office, Washington, D.C., pp. 731—759.

Roth, P.H., 1981. Mid-Cretaceous calcareous nannoplankton from the central Pacific: Implication for paleoceanography. In: Initial Reports of the Deep Sea Drilling Project, 62. U.S. Government Printing Office, Washington, D.C., pp. 471—489.

Roth, P.H., 1983. Calcareous nannofossils in mid-Cretaceous Black Shale Cycles from the Atlantic and Pacific: Effects of Diagenesis. Eos, 64: 733—734.

Roth, P.H., 1984. Preservation of calcareous nannofossils and fine-grained carbonate particles in mid-Cretaceous sediments from the southern Angola Basin. In: Initial Reports of the Deep Sea Drilling Project, 75. U.S. Government Printing Office, Washington, D.C., pp. 651—655.

Roth, P.H. and Berger, W.H., 1975. Distribution and dissolution of coccoliths in the south and central Pacific. Cushman Found. Foraminiferal Res., Spec. Publ., 13: 87—113.

Roth, P.H. and Bowdler, J.L., 1981. Middle Cretaceous calcareous nannoplankton biogeography and oceanography of the Atlantic Ocean. Soc. Econ. Paleontol. Mineral. Spec. Publ., 32: 517—546.

Roth, P.H. and Coulbourn, W.T., 1982. Floral and solution patterns in surface sediments of the North Pacific. Mar. Micropaleontol., 7: 1—52.

Roth, P.H. and Thierstein, H.R., 1972. Calcareous nannoplankton: Leg 14 of the Deep Sea Drilling Project. In: Initial Reports of the Deep Sea Drilling Project, 24. U.S. Government Printing Office, Washington, D.C., pp. 421—486.

Ryan, W.B.F. and Cita, M.B., 1977. Ignorance concerning episodes of ocean-wide stagnation. Mar. Geol., 23: 197—215.

Schlanger, S.O. and Jenkyns, H.C., 1976. Cretaceous oceanic anoxic events — causes and consequences. Geol. Mijnbouw, 55: 179—184.

Schwarzbach, M., 1974. Das Klima der Vorzeit. Enke, Stuttgart, 3rd Ed., 380 pp.

Sibuet, J.C., Ryan, W.B.F. et al., 1979. Initial Reports of the Deep Sea Drilling Project, 47, part 2. U.S. Government Printing Office, Washington, D.C., 787 pp.

Supko, P.R. and Perch-Nielsen, K. et al., 1977. Initial Reports of the Deep Sea Drilling Project, 39. U.S. Government Printing Office, Washington, D.C., 1139 pp.

Thierstein, H.R., 1973. Lower Cretaceous nannoplankton biostratigraphy. Abh. Geol. Bundesanst., (Wien), 29: 1—52.

Thierstein, H.R., 1980. Selective dissolution of late Cretaceous and earliest Tertiary calcareous nannofossils: experimental evidence. Cretaceous Res., 2: 1—12.

Thierstein, H.R. and Berger, W.H., 1978. Injection events in ocean history. Nature, 276: 461—466.

Thierstein, H.R. and Roth, P.H., 1980. Stable isotopes and biogeography of mid-Cretaceous microfossils. In: Abstr. 26th Int. Geol. Congr., Paris, 1980, p. 293.

Tissot, B., Deroo, G. and Herbin, J.P., 1979. Organic matter in Cretaceous sediments of the North Atlantic: Contribution to sedimentology and paleoceanography. In: M. Talwani, W. Hay and W.B.F. Ryan (Editors), Deep Drilling Results in the Atlantic Ocean: Continental Margins and Paleoenvironments. Am. Geophys. Union, Washington, D.C., pp. 362—374.

Tissot, B., Demaison, G., Masson, P., Delteil, J.R. and Combaz, A., 1980. Paleoenvironment and petroleum potential of Middle Cretaceous Black Shales in Atlantic Basin. Am. Assoc. Pet. Geol. Bull., 64: 2051—2063.

Tucholke, B.E., Vogt, P.R. et al., 1979. Initial Reports of the Deep Sea Drilling Project, 42. U.S.

Government Printing Office, Washington, D.C., 1115 pp.

Veevers, J.J., Heirtzler, J.R. et al., 1974. Initial Reports of the Deep Sea Drilling Project, 27. U.S. Government Printing Office, Washington, D.C., 1060 pp.

Wilde, P. and Berry, W.B.N., 1982. Progressive ventilation of the oceans-potential for return to anoxic conditions in the post-Paleozoic. In: S.O. Schlanger and M.B. Cita (Editors), Nature and Origin of Cretaceous Carbon-rich Facies. Academic Press, London, pp. 209—224.